Author's Personal Copy

Tectonophysics 608 (2013) 1049–1072

Contents lists available at ScienceDirect

Tectonophysics

journal homepage: www.elsevier.com/locate/tecto

Seismic velocity model of the crust and upper mantle along profile PANCAKE across the Carpathians between the Pannonian Basin and the East European Craton

V. Starostenko [a], T. Janik [b], K. Kolomiyets [a,*], W. Czuba [b], P. Środa [b], M. Grad [c], I. Kovács [d], R. Stephenson [e], D. Lysynchuk [a], H. Thybo [f], I.M. Artemieva [f], V. Omelchenko [a], O. Gintov [a], R. Kutas [a], D. Gryn [a], A. Guterch [b], E. Hegedűs [d], K. Komminaho [g], O. Legostaeva [a], T. Tiira [g], A. Tolkunov [h]

[a] Institute of Geophysics, National Academy of Sciences of Ukraine, Palladin Av. 32, 03680 Kiev, Ukraine
[b] Institute of Geophysics, Polish Academy of Sciences, Ks. Janusza 64, 01-452 Warsaw, Poland
[c] Institute of Geophysics, Faculty of Physics, University of Warsaw, Pasteura 7, 02-093 Warsaw, Poland
[d] Eötvös Loránd Geophysical Institute of Hungary, H-1145 Budapest, Hungary
[e] School of Geosciences, King's College, University of Aberdeen, Aberdeen AB24 3UE, UK
[f] Geology Section, IGN, University of Copenhagen, Øster Voldgade 10, DK-1350 Copenhagen, Denmark
[g] Department of Geosciences and Geography, Institute of Seismology, Gustaf Hällströmin katu 2B, P.O. Box 68, FIN-00014, University of Helsinki, Finland
[h] State Geophysical Enterprise "Ukrgeofizika", S. Perovskoy str. 10, 03057, Kiev, Ukraine

ARTICLE INFO

Article history:
Received 25 April 2013
Received in revised form 26 June 2013
Accepted 4 July 2013
Available online 11 July 2013

Keywords:
Pannonian Basin
Carpathians
East European Craton
Crust
Upper mantle
Seismic modelling

ABSTRACT

Results are presented of a seismic wide-angle reflection/refraction survey along a profile between the Pannonian Basin (PB) and the East European Craton (EEC) called PANCAKE. The P- and S-wave velocity model derived can be divided into three sectors: the PB; the Carpathians, including the Transcarpathian Depression and the Carpathian Foredeep; and the south-western part of the EEC, including the Trans European Suture Zone (TESZ). Seismic data support a robust model of the V_p velocity structure of the crust. In the PB, the 22–23 km thick crust consists of a 2–5 km thick sedimentary layer (V_p = 2.4–3.7 km/s), 17–20 km thick upper crystalline crust (5.9–6.3 km/s) and an up to 3 km thick lower crustal layer (V_p = 6.4 km/s). In the central part of the Carpathians, a 10–24 km thick uppermost part of the crust with $V_p \leq 6.0$ km/s may correspond to sedimentary rocks of different ages; several high velocity bodies (V_p = 5.35, 5.95 and 6.05 km/s) within the sedimentary flysch sequences may represent volcanic sequences. The Moho depth changes from 25 km to 45 km over ca. 100 km distance beneath the Carpathians, west of TESZ. The cratonic crust has a typical three layer structure with a pronounced thickening of the lower crust towards the Ukrainian Shield, where a high velocity lower crust ($V_p > 7.2$ km/s) is observed. Two low-velocity lenses in the upper crust of the EEC are interpreted beneath major sedimentary troughs (Lviv and Volyn-Podolsk). Mantle reflectors are observed at depths of ~45 km and ~75 km below the PB and 10–20 km below the Moho in the EEC. Sub-Moho (Pn) velocities increase from 8.0 km/s beneath the PB to 8.1 km/s beneath the Carpathians and to ~8.3 km/s beneath the EEC. S-waves of acceptable quality are recorded in the EEC; their signal-to-noise ratios increase towards the Ukrainian Shield.

© 2013 Elsevier B.V. All rights reserved.

1. Introduction

The results of a seismic wide-angle reflection/refraction (WARR) survey along the PANCAKE (PANnonian-CArpathians-Cratonic Europe) profile across the Pannonian Basin in Hungary, the Ukrainian segment of the Eastern Carpathian orogen and the south-western part of the East European Craton are presented. PANCAKE was organised as the third profile of a series of WARR profiles in Ukraine, following DOBRE'99 (DOBREfraction'99 Working Group et al., 2003; Grad et al., 2003a) which targeted the Donbas Foldbelt, and project DOBRE-2 (Starostenko et al., 2008; Tolkunov et al., 2011) along the Azov Massif–Azov Sea Kerch Peninsula–eastern Black Sea line.

The PANCAKE profile (Fig. 1) is 645 km long, with 157 km in Hungary and 488 km in Ukraine. In the vicinity of the PANCAKE profile, early Soviet deep seismic sounding (DSS) profiles — Geotraverses II, IV and VI (Fig. 1) — were acquired in the 1970s–1980s (Sollogub et al., 1988) and a part of the adjacent East European Craton was investigated by the EUROBRIDGE project (EUROBRIDGE Seismic Working Group, 1999; Thybo et al., 2003). Geotraverse II imaged the deep structure of the Carpathians, Carpathian Foredeep and Transcarpathian Depression along a profile parallel to and in the vicinity of the PANCAKE profile

* Corresponding author. Tel.: +380 444240100; fax: +380 444502520.
E-mail address: katls@igph.kiev.ua (K. Kolomiyets).

0040-1951/$ – see front matter © 2013 Elsevier B.V. All rights reserved.
http://dx.doi.org/10.1016/j.tecto.2013.08.004

Author's Personal Copy

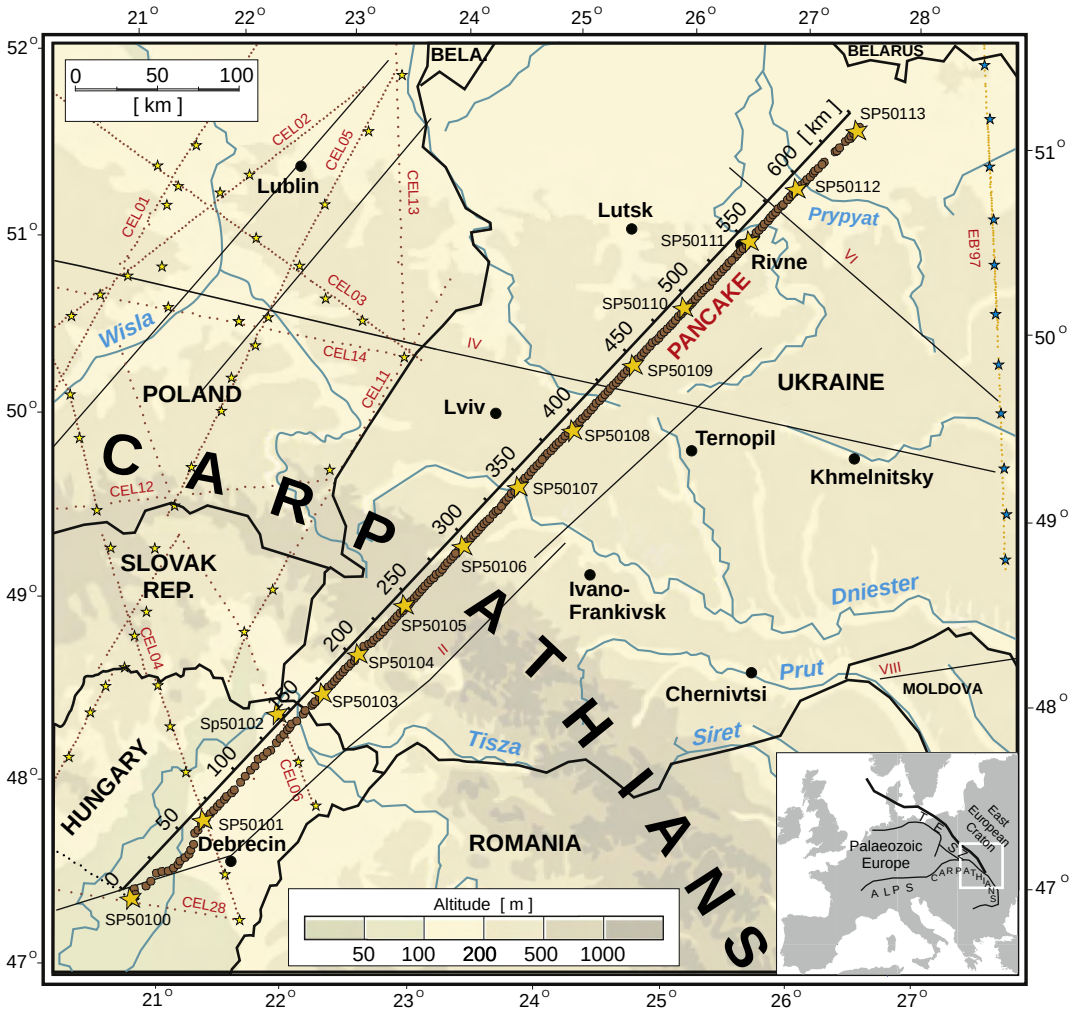


Fig. 1. Location of main seismic experiments in the study area and location of the investigated PANCAKE profile. Stars represent the shot points and red dots represent recording stations of WARR experiments; black lines represent older DSS profiles. Inset map shows the location of target area in the Europe.

(Sollogub et al., 1988). However, this survey focused mainly on interpretation of reflected phases and provides only limited velocity information. South and west of the study area, the structure of the Carpathians and of the Pannonian Basin was recently studied within the scope of the CELEBRATION 2000 experiment (Guterch et al., 2001). In the Pannonian Basin, several refraction and deep reflection profiles were recorded in 1980s (Posgay, 1988; Posgay et al., 1995).

The PANCAKE experiment was designed to provide a detailed model of the seismic P-wave velocity structure of the crust and uppermost mantle in this area, with the aim of constraining the tectonic and geodynamic evolution of the Pannonian Basin and the complex boundary between the Eastern European Craton and the Carpathians. Specific targets are crustal affinity and structure of the transition zone between the East European Craton and adjacent crustal units underlying the Carpathian orogen and the Pannonian Basin, as well as the architecture of overlying sedimentary layers, given that the study area is believed to have a significant hydrocarbon potential.

2. Geological and tectonic setting

From north-east to south-west, the profile crosses the south-western edge of the East European Craton (EEC), the Eastern Carpathian orogen, the ALCAPA (Alps–Carpathians–Pannonian) micro-plate, and partly the Tisza-Dacia micro-plate, which borders the ALCAPA along the Mid Hungarian tectonic zone (Csontos and Nagymarosy, 1998; Figs. 2, 3). These tectonic units, having ages ranging from Archaean to Quaternary, also have different geological origins, lithosphere structure, and geodynamic history.

Within the EEC (at profile distances of km 650–340), the profile crosses the following structural elements (Glushko and Kruglov, 1988; Gursky and Kruglov, 2004; Khain and Leonov, 1998) from NE to SW (Fig. 2): the south-western slope of the Ukrainian Shield (km 620–650), the Volyn-Polesie Trough (km 540–620), the Volyn-Podolian Monocline (km 490–540), and the Palaeozoic Lviv Trough (km 340–490). Further south-west, the PANCAKE profile crosses the Eastern Carpathians (km 160–340), which are subdivided into two tectonic units separated by regional thrusts: the Carpathian Foredeep (km 290–340) which overlies the Trans-European Suture Zone (TESZ)and the Outer (Folded or Flysch) Carpathians (km 200–290). At the south-western end (km 0–160) the profile crosses the Pannonian Basin.

The TESZ, at the SW border of the EEC beneath the sediments of Carpathian Foredeep and the Skyba nappe (km 160–340), includes the crustal units separating the “ancient” Precambrian Europe from the Variscan and Alpine orogens (Berthelsen, 1993). It is understood here as the area which includes the Neoproterozoic/Palaeozoic units overlying the thinned EEC margin and separates the EEC from the Outer Carpathians in the SW. The Carpathian Foredeep consists of Neogene molasse, comprising the outer-autochthonous and almost

Author's Personal Copy

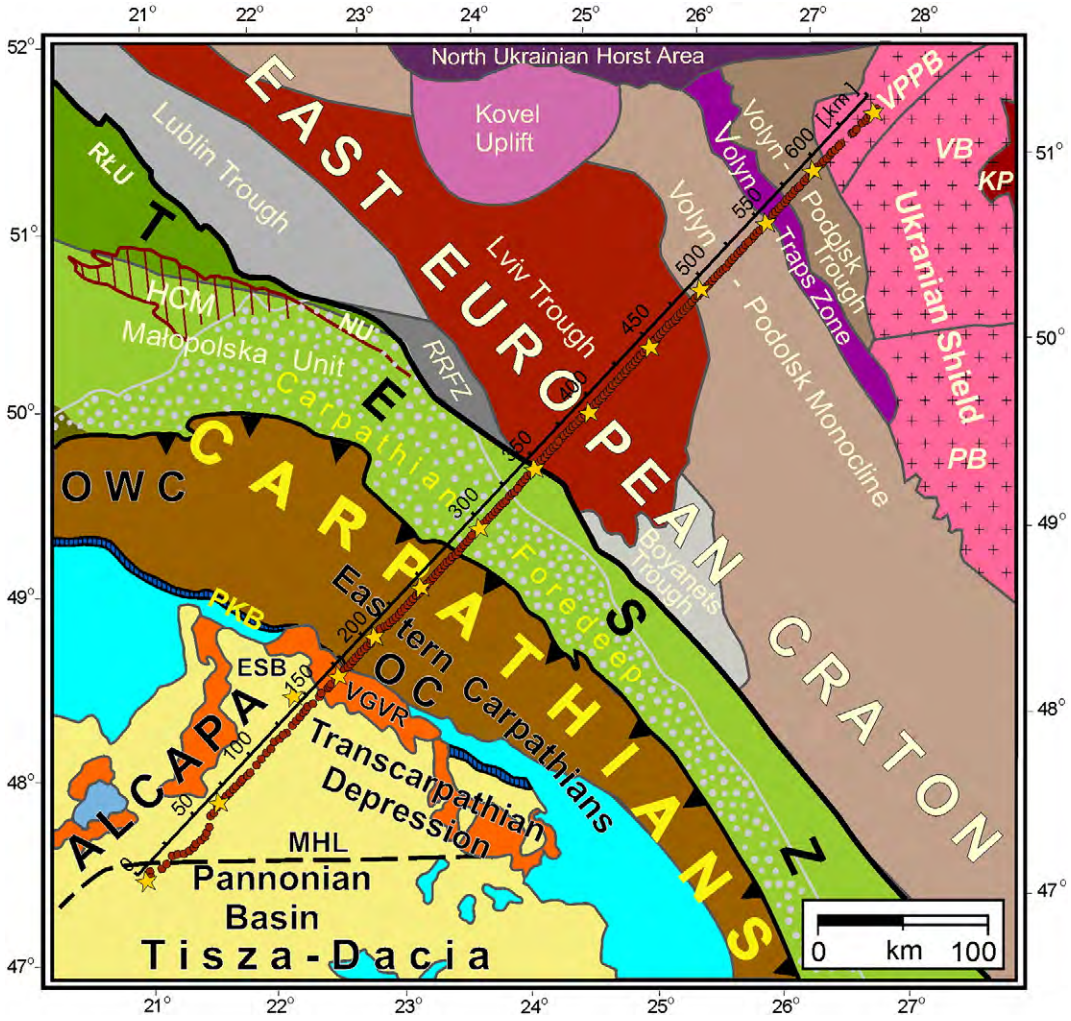


Fig. 2. Schematic tectonic map of the research area (as in Fig. 1). PB — Podolian Block; ESB — East Slovakian Basin; HCM — Holy Cross Mountains; KP — Korosten Pluton; MHL — Mid Hungarian Line; NU — Narol Unit; OC — Outer Carpathians; OWC — Outer West Carpathians; PKB — Pieniny Klippen Belt; RŁU — Radom-Łysogóry Unit; RRFZ — Rava Ruska folded zone; TESZ — Trans-European Suture Zone; VB — Volyn Block; VGVR — Vygorlat-Guta Volcanic ridge; VPPB — Volhyn-Polesie Plutonic Belt. Black lines with black triangles represent main trusts, blue areas filled black lines represent Pieniny Klippen Belt, cyan areas represent inner Carpathian–Alpine units, orange areas represent Neogene volcanics. Solid black line represents the edge of East European Craton.
The map modified after Dadlez (2003), Dadlez et al. (1994), Fodor et al. (1999), Glushko and Kruglov (1988), Gursky and Kruglov (2004), Janik et al.(2009), Kováč (2000), Kováč et al. (1994), Środa et al.(2006).

non-deformed Miocene sedimentary unit deposited on the Palaeozoic–Mesozoic cover of the EEC and the TESZ, and the internal allochtonous zone (the Sambor and Boryslav-Pokut nappes).

The Outer (Flysch) Carpathians form a system of linear imbricated structures, overturned and thrust over the Carpathian Foredeep by more than 10 km. The Pieniny Klippen Belt (PKB) separates the Outer Carpathians from the Inner Carpathians and the Transcarpathian Depression. The PKB is a typical tectonic mélange thrust towards the Outer Carpathians (Kruglov et al., 2007). Large blocks of Jurassic and Lower Cretaceous limestones are embedded in an Upper Cretaceous marly matrix, in the near-surface layers in a 10 km wide zone.

The origin of the Carpathian–Pannonian region is still debated. According to some authors (e.g. Fodor et al., 1999; Horváth, 1993) it was formed in the Tertiary as the result of subduction of oceanic lithosphere beneath the ALCAPA and the Tisza-Dacia micro-plates and the closure of the residual Magura Ocean between them and the EEC. Alternative views on the formation of the Pannonian Basin (PB) include subsidence associated with rifting (Huismans et al., 2001), with asthenospheric flow triggered by the Europe–Africa collision (Cloetingh et al., 2004; Kovács et al., 2012) or with gravitational instability and possible lithosphere downwelling (Gemmer and Hauseman, 2007).

Since the PB is covered by Miocene–Pliocene sediments of varying thickness (from 0 to 4 to 6–7 km), the lateral extent and structure of the pre-Tertiary basement of the north-eastern part of the ALCAPA micro-plate is unknown. The pre-Tertiary basement, where sampled by drill cores penetrating the thick Tertiary sedimentary cover, is composed mainly of Mesozoic carbonaceous sediments (Kovács et al., 2000).

3. Seismic data

The field acquisition campaign took place in October 2008 and included 14 explosive sources (shot points — SP — see Table 1 for details) at 35–50 km distance (3 in Hungary and 11 in Ukraine), and 261 recording stations with one-component geophones placed every ~2.5 km.

The seismic phases that were correlated and used for modelling include, as first arrivals, refractions from the sedimentary layers (P_{sed}), diving and refracted arrivals from the upper/middle crystalline crust (P_g), and refractions from the upper mantle (P_n). The signal-to-noise ratio is good to 150 km offsets in the Pannonian Basin (PB) and to 300 km in the East European Craton (EEC). Among the secondary arrivals, the strongest phase is the reflection from the Moho discontinuity (P_MP). Reflections from mid-crustal discontinuities (P_CP) are also

Author's Personal Copy

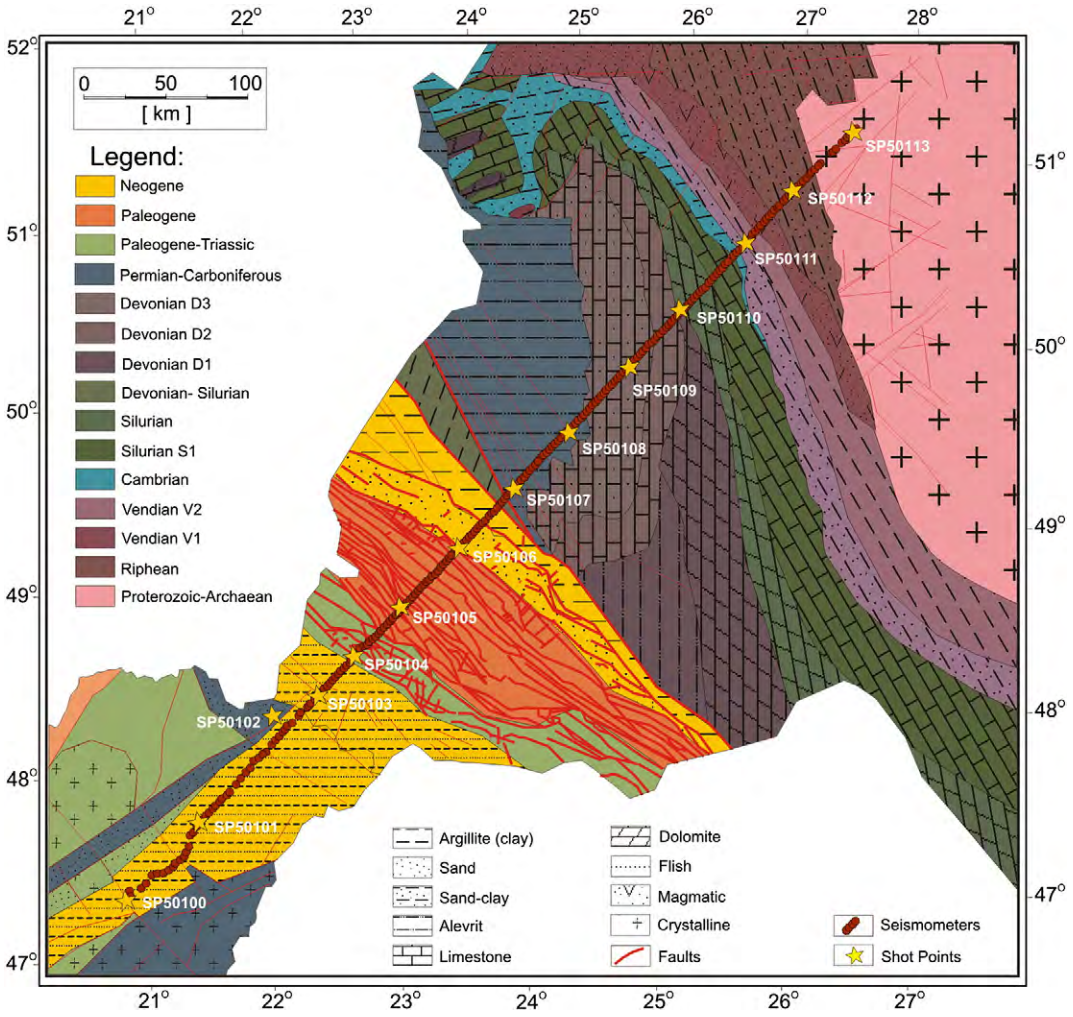


Fig. 3. Geological map of the study area, covering the same area as Fig. 1.
Eastern Hungary after Fulop and Dank (1987) and western Ukraine and Moldova after Zaritsky (1987).

observed in some shot records. At large offsets, reflected phases from the upper mantle (P_1P) are identified in several sections. Seismic record sections show a variable wavefield character, reflecting differences in the structure of individual tectonic units along the profile.

3.1. P-waves

In the seismic data from the Pannonian Basin area (shot points 50100–50104), the P_{sed} phases are usually observed in the offset range of approx. 0–15 km, with apparent velocities of 4.5–5.5 km/s (Fig. 4). At larger distances (15 km to 50–80 km), the P_g phase is observed. Its apparent velocity (commonly 6.0 km/s, sometimes 5.7 km/s) suggests that it is a refraction (turning wave) from the crystalline basement of the PB. The uppermost mantle refraction (P_n) has low amplitude (see zoom of SP50101, Fig. 4) or is invisible in this area. In the later arrivals, a clear Moho reflection (P_MP) phase can be correlated at about 6 s, with maximum amplitude at offsets of 50–80 km, which suggests a relatively thin crust (<30 km). Intracrustal reflections are not observed. In

Table 1
Location and parameters of explosive sources used along the PANCAKE profile.

Shot point number	Distance (km)	Latitude N φ (deg)	Longitude E λ (deg)	Altitude h (m)	Time UTC (y:d:h:m:s)	Charge TNT (kg)
SP50100	0	47.30079	20.83466	92	2008:288:21:00:02.07	700
SP50101	64.770	47.71834	21.43426	96	2008:289:21:00:23.04	400
SP50102	143.098	48.28246	22.06985	100	2008:290:20:33:11.00	300
SP50103	170.543	48.38278	22.44973	106	2008:288:20:00:00.00	389
SP50104	202.788	48.58875	22.75683	601	2008:288:21:30:00.00	600
SP50105	243.680	48.84234	23.15927	738	2008:289:20:00:00.00	600
SP50106	294.366	49.1476	23.67389	389	2008:290:21:30:00.00	600
SP50107	343.740	49.45165	24.16854	286	2008:290:20:00:00.00	588
SP50108	391.661	49.74	24.66112	395	2008:290:21:00:00.00	560
SP50109	445.877	50.07056	25.21583	235	2008:291:20:00:00.00	700
SP50110	492.617	50.36361	25.68583	197	2008:290:22:00:00.00	700
SP50111	549.744	50.69417	26.30278	170	2008:289:20:29:55.99	800
SP50112	592.638	50.955	26.75139	164	2008:289:21:29:50.05	800
SP50113	643.727	51.23753	27.32736	184	2008:288:22:00:00.00	1000

Author's Personal Copy

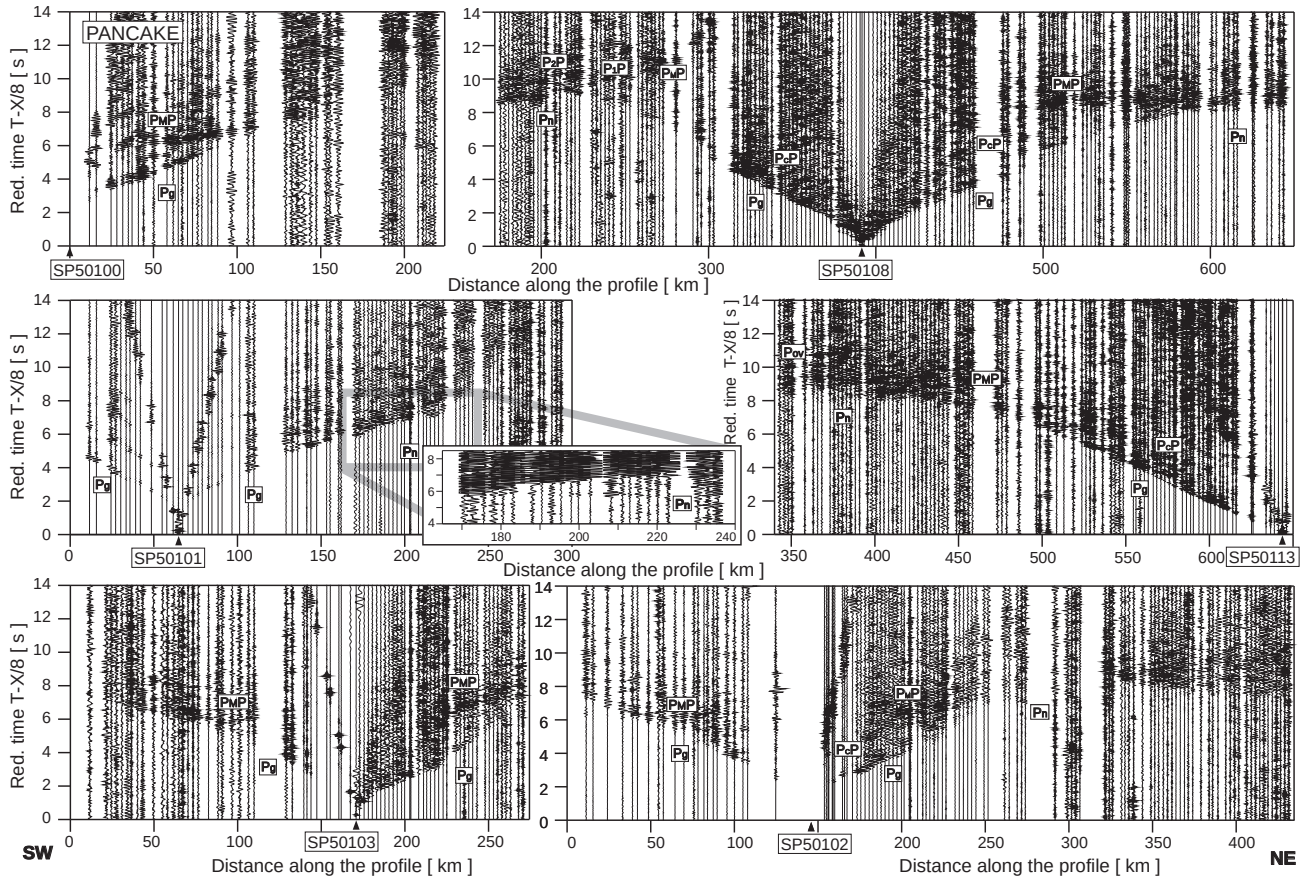


Fig. 4. Example of trace-normalized, vertical-component seismic record sections for P-wave along the PANCAKE profile (SP50100, SP50101, SP50102, SP50103, SP50108, SP50113) filtered by a band-pass filter (2–15 Hz). Abbreviations: Pg — seismic refractions from the upper and middle crystalline crust; Pov — overcritical crustal phases; PcP — reflections from the middle crust discontinuities; P_MP — reflected waves from the Moho boundary; Pn — refractions from the sub-Moho upper mantle; P_1P — P-wave phases from the upper mantle. The reduction velocity is 8.0 km/s.

the PB, the observed phases have short pulses with no coda, especially in the south (e.g., SP50100 and SP50101, Fig. 4). This implies a relatively transparent crust with no pronounced reflectivity between possible discontinuities.

Most of the Outer Carpathians and the Carpathian Foredeep is characterized by low apparent velocities of phases from the sedimentary layer — about 4.5–5.5 km/s (P_{sed}), while velocities of about 6.0 km/s, corresponding to P_g, are usually not observed. This is ascribed to effects of the more than 15 km thick low velocity sediments comprising the Carpathian orogen and the Carpathian Foredeep as well as underlying Palaeozoic to Mesozoic metasediments which may damp seismic phases from the crystalline basement. In several record sections, some short branches of travel times with apparent V_p of ~6.0 km/s are observed at offsets of about 20 km. This suggests the existence of thin high velocity bodies within the sedimentary layer. This area also shows strong attenuation of seismic waves, probably due to the presence of heavily deformed and fractured sediments. For some shot points, e.g., SP50105 and SP50106, the seismic signal is recorded only to offsets of 50 km or less. Also, first arrivals are usually ringing and the later wavefield shows long, random reflectivity, obscuring any possible later arrivals. Moho reflections are usually very weak compared to the background wave field, or not visible at all. The P_n phase from the Carpathian area is observed only for shot points located outside this area — e.g., SP50104 and SP50108. At large offsets (over 200 km), high apparent velocity (>8.0 km/s) arrivals for the SW branches of SP50108 and SP50109 (Figs. 4 and 5), and ~8.0 km/s (SP50102, Fig. 4) are observed, most likely representing reflections from upper mantle discontinuities.

In the EEC, the offset range of P_{sed} (V_p of 4–5.5 km/s) decreases from ~15 km in the south to 0 km in the north, indicating thinning of the EEC sedimentary cover. P_g in this area has high signal-to-noise ratio and can be easily correlated at offsets up to 150–200 km. Its apparent velocity is in 6.0–6.2 km/s range (Figs. 4 and 5). In the south-west, the P_g arrivals are usually followed by a long coda, suggesting substantial reflectivity of the crust, while in the north-east the crust seems to be more transparent with sharp P_g arrivals followed by a low-amplitude signal. In several locations, the P_g phase shows a strong decrease of amplitude with offset, resulting in gaps in the travel time curve, typical for the presence of a low velocity zone (LVZ). For SP50107 and SP50108, a gap at 15 km offsets suggests a LVZ in the uppermost crust. Shot points 50108 and 50110 show an amplitude decrease of a P_g phase at ~80 km offset that may be due to a LVZ (or a zone with low velocity gradient) in the upper/middle crust. For most of the shot points in the EEC, reflections from the upper crust can be correlated (e.g., SP50110–50113, Figs. 4 and 5). In some sections, good quality Moho reflections and refractions are observed, e.g. SP50108 and 50112. The P_MP critical point (point of maximum amplitude) at ~150 km offset and relatively late arrival time (~8 s reduced time) indicate a >45 km thick crust beneath the EEC. For some shot points, well-developed overcritical Moho reflections, most likely merging with deeper crustal phases ($P_{ov}P$), can be correlated up to offsets of 200–300 km (cf. for SP50109 and SP50113; Figs. 4 and 5).

3.2. S-waves

The S-wave arrivals have lower signal-to-noise ratio than the P-waves. The onsets are often obscured by the P coda and are hard

Author's Personal Copy

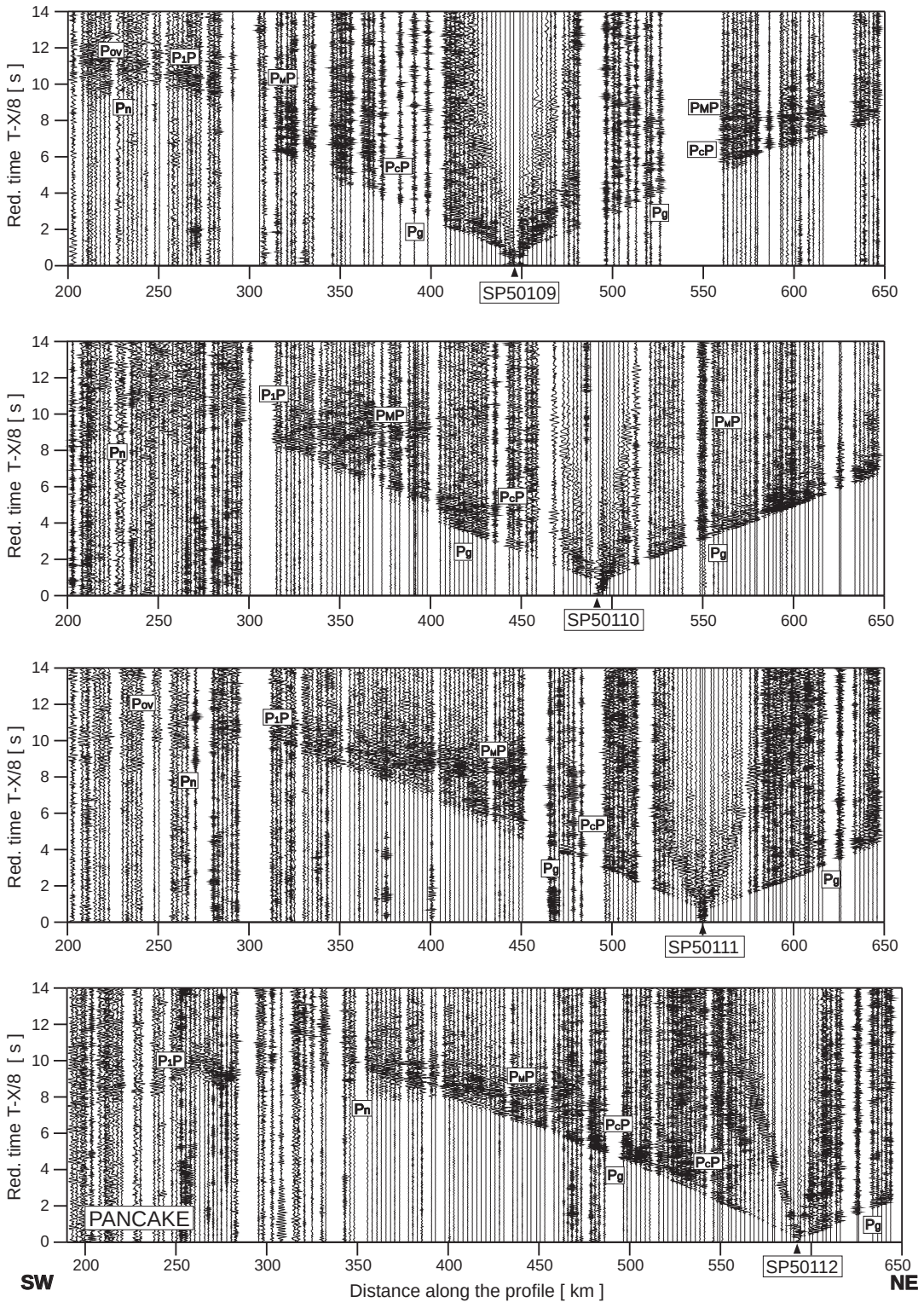


Fig. 5. Example of trace-normalized, vertical-component sections for P-waves along PANCAKE profile (SP501009, SP5010102, SP501011, SP501012) filtered by a band-pass filter (2–12 Hz). Abbreviations are as in Fig. 4.

to pick consistently. S-waves of acceptable quality are recorded in the EEC (northeastward from SP50107 and SP50108) with increasing signal-to-noise ratio towards the northern end of the profile (see SP50111, SP50112 and SP50113; Fig. 6). The only visible phases are the S_g phase, observed to offsets 70–100 km with apparent velocities of 3.5–3.6 km/s, a few crustal reflections and the S_MS phase, with critical point at ~150 km offset (Fig. 5).

4. Seismic modelling

The interpretation of the seismic data includes ray-tracing forward modelling followed by modelling of the amplitudes of the recorded phases with finite-difference, full waveform synthetic seismograms. The trial-and-error forward modelling is carried out using the ray-tracing SEIS83 package (Červený and Pšenčík, 1984)

Author's Personal Copy

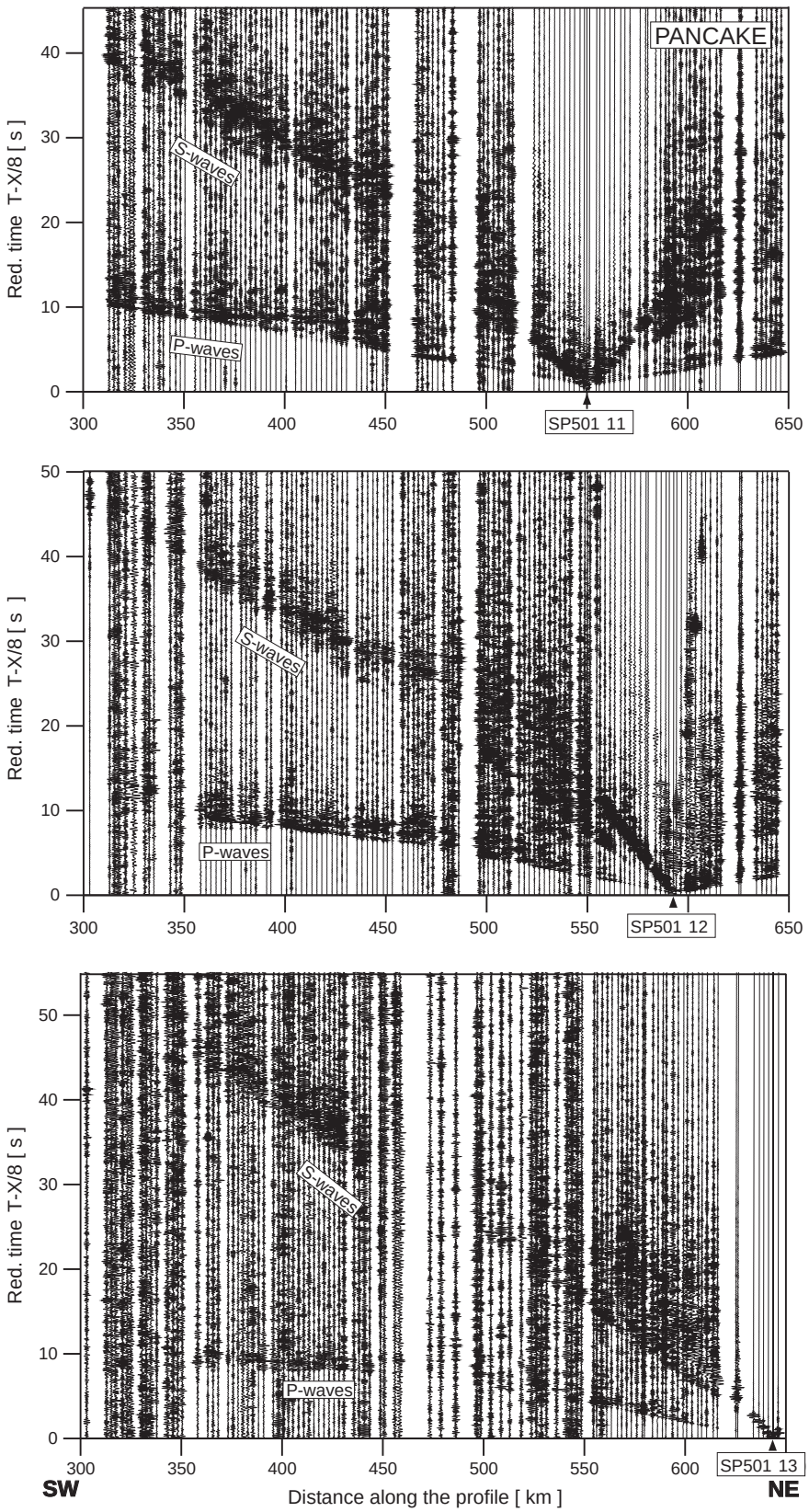


Fig. 6. Example of trace-normalized, vertical-component, common seismic record sections for P- and S-waves along PANCAKE profile (SP501011, SP501012, SP501013) filtered by a band-pass filter (1–8 Hz).

supplemented with the graphical interface MODEL (Komminaho, 1998) and ZPLOT (Zelt, 1994). The algorithm calculates ray paths, travel times and synthetic seismograms with a high frequency approximation. The model consists of layers with smoothly varying velocities, separated by discontinuities. In each layer, the P-wave velocity is parameterized on an irregular rectangular grid and interpolated by bicubic splines. In this study, geological and geophysical data from over a dozen boreholes located near the profile and

Author's Personal Copy

velocity data from shallow seismic reflection and refraction investigations are used, when available, to constrain the velocity distribution in the sedimentary strata of the uppermost crust for definition of an initial model. The model is iteratively modified in order to minimize the travel time misfit and to obtain similar amplitudes of synthetic and observed data, given that amplitude provides important constraints on the velocity gradients and contrasts at the discontinuities (Fig. 7). Examples of ray-tracing forward modelling are shown in Figs. 8–17.

Full waveform synthetic sections are calculated with the finite-difference Tesseral 2-D package (Kostyukevich et al., 2000). The final ray-tracing velocity model is transformed onto a grid with 500 m spacing horizontally and 100 m vertically. The S-wave velocities are obtained from values of V_p/V_s ratio as derived by the ray-tracing

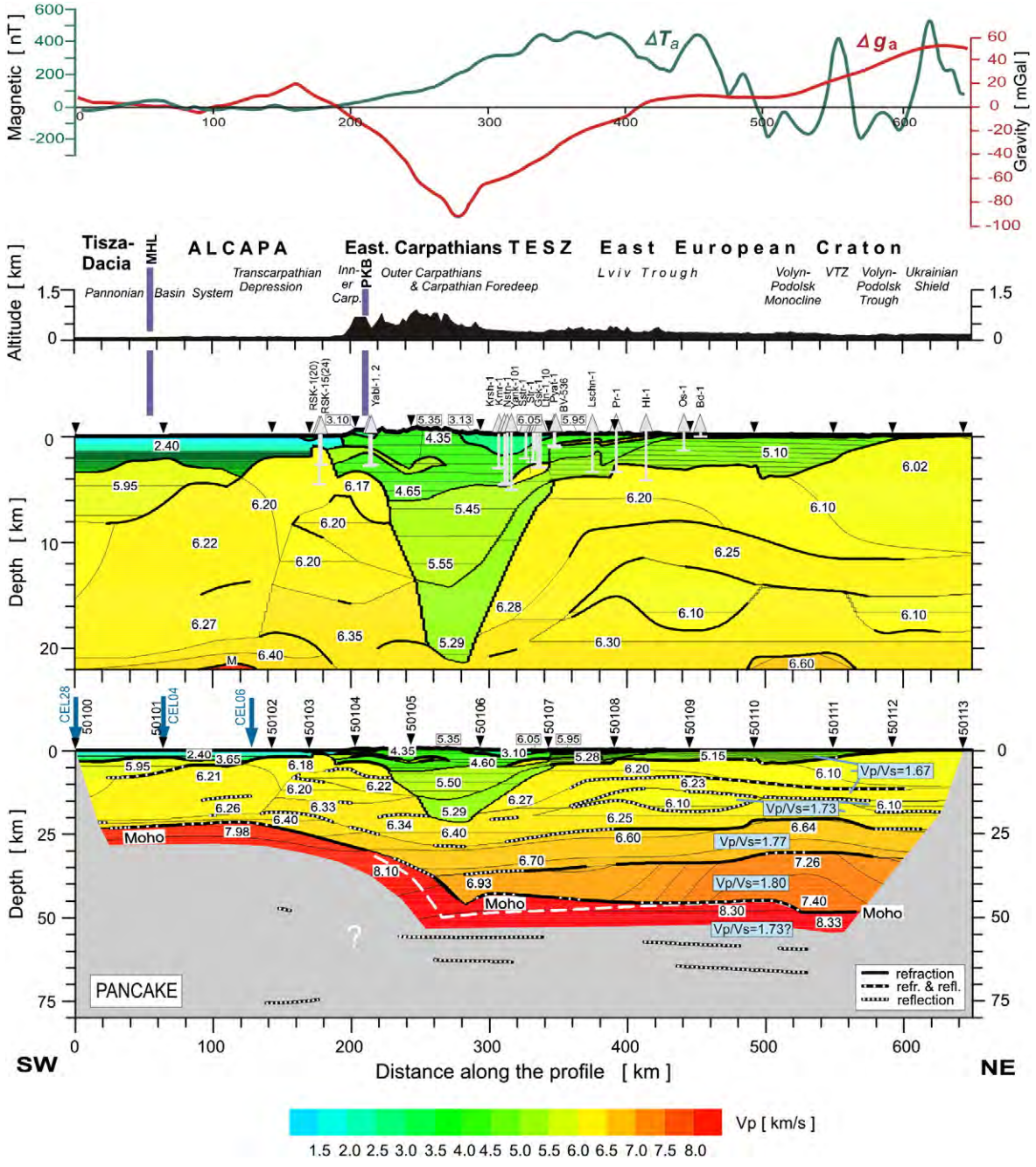


Fig. 7. Two-dimensional model of seismic P-wave velocity in the crust and upper mantle derived by forward ray-tracing modelling using the SEIS83 package (Červený and Pšenčík, 1984) along the PANCAKE profile (bottom diagram). Thick, black lines represent major velocity discontinuities (first order interfaces). Those parts of the first order discontinuities that have been constrained by reflected or/and refracted arrivals of P-waves are marked by thick lines. Thin lines represent velocity isolines with values in km/s shown in white boxes. Locations of large-scale crustal blocks are indicated. Arrows show positions of shot points. Blue arrows show intersections with other profiles. Vertical exaggerations are ~8.3:1 for upper part of the model, and ~2.4:1 for whole model. For the EEC, model of V_p/V_s ratio distribution is shown. The white dashed line represents depth of the Moho boundary if a velocity ~7.2 km/s is used instead of 6.9 km/s in the lower crust. MHL — Mid Hungarian Line; PKB — Pieniny Klippen Belt; VTZ — Volyn Traps zone; M — Moho boundary. Bouguer gravity and total magnetic field anomalies along the PANCAKE profile are shown on top diagrams (Khomenko, 1987; Kruglov, 2001). Boreholes: Rsk-20, 1, 15, 24 — Ruski Komarivtsi-20, 1, 15, 24 (15 km to NW from the profile; 10 km to SE; 9 km to NW, respectively); Yabl-1, 2 — Yablunivska-1, 2 (20 and 22 km to SE); Krsh-1 — Krushelnitska-1 (3 km to SE); Kmr-1 — Komarnytska-1 (7.5 km to NW); Nstn-1 — Nyzhnyostynavska-1 (1,5 km to NW); Yank-101 — Yankivska-101 (8.5 km to SE); Sstr-1 — South-Stryiska-1 (0.5 km to SE); Str-1 — Stryiska-1 (1 km to NW); Gsk-9 — Gaiska-9 (6 km to NW); Ltn-1 — Lyutnianska-1 (15 km to NW); Ltn-10 — Lyutnianska-10 (17 km to NW); Pyat-1 — Pyatichnska-1 (1 km to NW); BV-536 — Bilche-Volytska-536 (0.1 km); Lschn-1 — Lischynska-1 (11 km to SE); Pr-1 — Peremyshiany-1 (7 km to SE); Hl-1 — Hlyniany-1 (24 km to NW); Os-1 — Olesko-1 (7 km to NW); Bd-1 — Brody-1 (8.5 km to NW).

Author's Personal Copy

modelling. For the cratonic part of the model, where the quality of S-wave record sections is high, values of the V_p/V_s ratio are adequately defined. For other parts of the model (SW and central) V_p/V_s values from the cratonic part are used. The P-wave and S-wave grids make the input model for full waveform computations. As for the ray-tracing modelling, the surface topography is taken into account.

The dominant frequency of the source impulse is 10 Hz, which allowed performing calculations with such a large model in a reasonable time, given the available computation resources and avoiding spatial aliasing and numerical instability. Due to the large volume of input data, the computations were performed on a grid of computers using parallel computation capabilities (Kolomiyets and Kharchenko, 2008). Full waveform modelling allows simulation of the wave propagation through the modelled structure such that all wave transformations (reflection, refraction, reverberations, etc.) at the main boundaries in the model can be visualised through time as a series of snap shots of the wave propagation through the model (Fig. 10). A good agreement between the observed records and the full waveform synthetic sections supports the veracity of the ray-tracing model. Comparison of the calculated full waveform synthetic sections with seismic record sections as well as the ray diagrams for SP50100, SP50104, SP50107, SP501010, SP501011 and SP501012 is presented in Figs 9, 11–13, 16 and 17, respectively.

5. P-wave model

Forward modelling of all 14 seismic record sections produced a velocity model of the crustal structure along the PANCAKE profile (Fig. 7). Sample documentation of the results of the 2D modelling for different parts of the profile is shown in Figs. 8–17. The region may be divided into three main crustal segments, based on the velocity structure and geological considerations. From the south-west to the north-east, these comprise: (i) the Pannonian Basin, the Transcarpathian Depression and the Inner Carpathians; (ii) the Outer Carpathians, the Carpathian Foredeep, including the TESZ; and (iii) the EEC, including Precambrian and Neoproterozoic/Palaeozoic units.

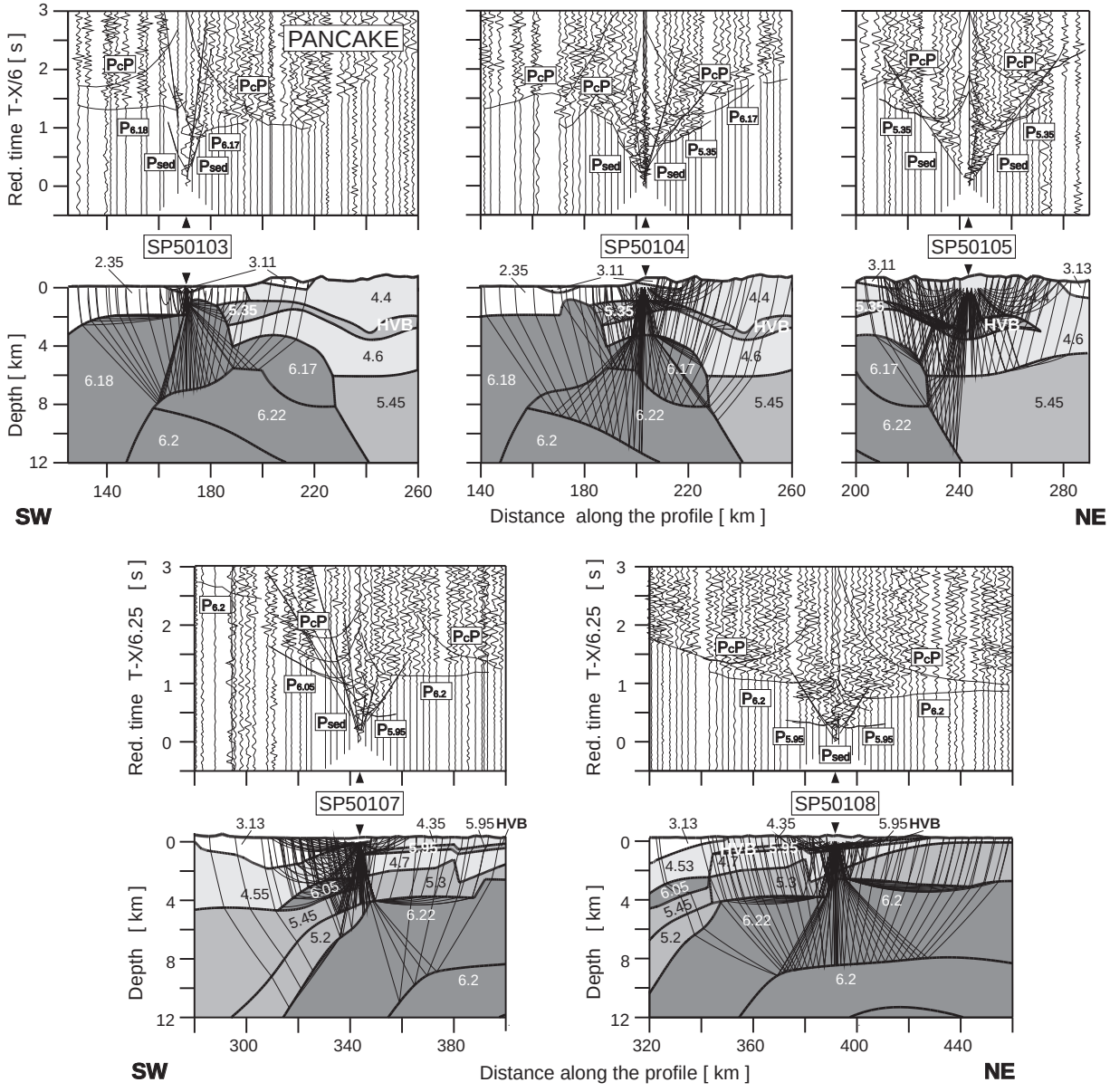


Fig. 8. Examples of details (high velocity bodies — HVB) of seismic modelling along the PANCAKE profile for SP50103, SP50104, SP50105, SP50107 and SP50108; seismic record sections of P-wave with theoretical travel times and ray diagram of selected rays calculated using the SEIS83 ray-tracing technique. P-wave data have been filtered using the band-pass filter of 2–15 Hz and displayed using the reduction velocity of 6.0 km/s or 6.25 km/s. All examples were calculated for the model presented in Fig. 7. Other abbreviations are as in Fig. 4.

Author's Personal Copy

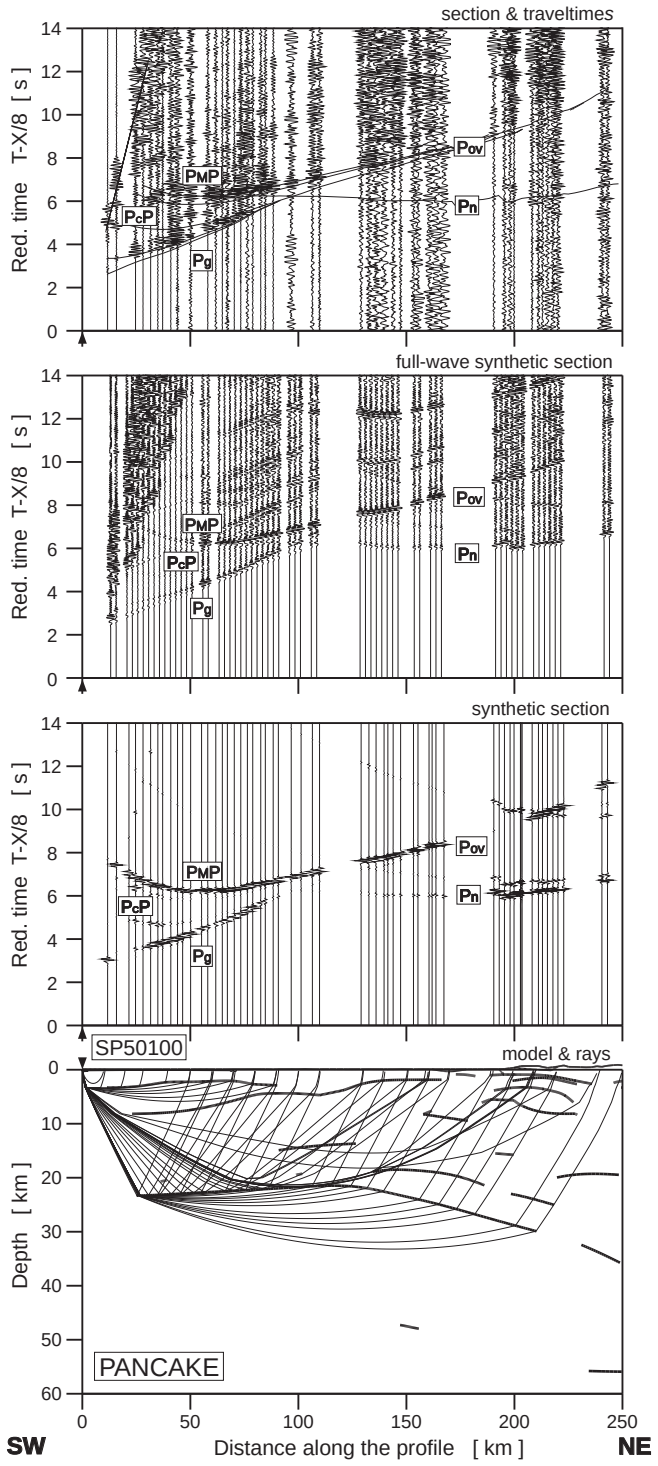


Fig. 9. Example of seismic modelling along the PANCAKE profile, SP50100; seismic record sections (amplitude-normalized vertical component) of P-wave with theoretical travel times calculated using the SEIS83 ray-tracing technique. P-wave data have been filtered using the band-pass filter of 2–15 Hz and displayed using the reduction velocity of 8.0 km/s. Full-wave synthetic seismograms (second diagram) using TESSERAL program (Kostyukevich et al., 2000). Synthetic seismograms (third diagram) and ray diagram of selected rays using the SEIS83 (bottom diagram). All examples were calculated for the model presented in Fig. 7. Other abbreviations are as in Fig. 4.

5.1. Crustal velocity structure

5.1.1. Profile distance km 0–220

In the south-western part of the profile, only the Moho and the top of the basement can be detected as velocity discontinuities in the Earth's crust of the Pannonian Basin. The crust of the Pannonian Basin (km 0 to ~160 of the profile) is approximately 22–23 km thick and includes 2–5 km of sedimentary sequences (V_p = 2.4–3.7 km/s) underlain by a layer with V_p = 5.95 km/s, interpreted as being formed by folded Meso-Cenozoic sediments (Fig. 7). The thickness of the latter decreases from ca. 6 km in the SW to ca. 2 km towards the Transcarpathian Depression. Accordingly, the top of the probable Palaeozoic basement (V_p = 6.21 km/s) shallows to the north-east from 8 to 3–4 km depth. The upper crystalline crust with velocities of 5.9–6.3 km/s is underlain by a thin (1–3 km) crustal layer with V_p = 6.4 km/s (Figs. 9, 11, 13, 14). Further northeast, the metamorphosed Upper Palaeozoic volcanic complex (reached by boreholes near the PANCAKE profile), overlain by Neogene and Palaeogene formations, forms the basement of the Transcarpathian Depression with the top at a depth of about 3 km. In the Transcarpathian Depression the depth to Moho is the same as in the Pannonian Basin (ca. 22–23 km) and gradually increases to ca. 30 km north-eastwards beneath the Inner Carpathians and the Pieniny Klippen Belt, mostly due to thickening of the basal crustal layer with V_p = 6.4 km/s. The average basement velocities of the Pannonian Basin and the Transcarpathian Depression are ca. 6.07 km/s and 6.24 km/s, respectively. The lower crustal layer with velocities typical of the continental mafic crust is absent beneath both tectonic units.

The mélange zone of the Pieniny Klippen Belt is not clearly resolved by the PANCAKE seismic data. It has a block structure with possible different velocities in the constituent blocks as indicated by the presence of a high velocity body at a depth of ~4 km (km 200–210) near SP50104 (Fig. 8). The 7000 m deep borehole Synevydne 1, nearest to the profile in this area (km ~270), did not reach the basement below the flysch deposits (Lyzun and Zayats, 1997).

5.1.2. Profile distance km 220–380

Much of the Eastern Carpathians are characterized by the presence of a 10–24 km thick upper part of the crust with relatively low velocity (3.10 to 5.50 km/s) which may correspond to sedimentary rocks of the Carpathian orogen and may possibly include a part of its Neoproterozoic to Mesozoic basement. The largest sequence of sediments (ca. 20–21 km) is along the western margin of the TESZ is (Fig. 7) at km 280–290, which corresponds to the western margin of the Carpathian Foredeep. The uppermost layers (V_p = 3.10–4.60 km/s) with thickness 2 to 7 km and dip of 5–7° towards the southwest may correspond to the Carpathian flysch unit penetrated by boreholes in the region. Several high velocity bodies (with V_p = 5.35 km/s, 5.95 km/s and 6.05 km/s), identified within the interpreted Carpathian flysch strata (Fig. 7), may represent magmatic intrusions (e.g. Thybo and Schonharting, 1991). Further northeast (km ~290–350), the 3.10 km/s layer, reaching ~2 km in thickness, is interpreted as Miocene deposits of the Carpathian Foredeep.

The uppermost part of the basement below the Carpathian flysch sediments has V_p = 5.50 km/s. Interestingly, this layer is underlain by a lower velocity layer (V_p = 5.29 km/s). The latter may represent sedimentary cover deposited on the thinned crystalline crust of a similar (Proterozoic–Palaeozoic) age as the overlying layer (possibly thrust over the cover) but of a different lithology and/or of a lower metamorphic grade. Similar velocities (5.25 km/s) at similar depths were measured in the basement of the Carpathian orogen along the CEL05 profile (Grad et al., 2006a).

Below the lower velocity layer (V_p = 5.29 km/s), the crust of the Carpathians orogen to the north-east from km 260 has a three-layer structure typical of cratonic crust with an approximately equal thicknesses (ca. 8 km) of the felsic upper crust (V_p ~ 6.4 km/s), middle crust (V_p ~ 6.7 km/s) and mafic lower crust (V_p ~ 6.93 km/s). The lower crustal layer is absent beneath the western part of the orogen (southwest of km 260).

Author's Personal Copy

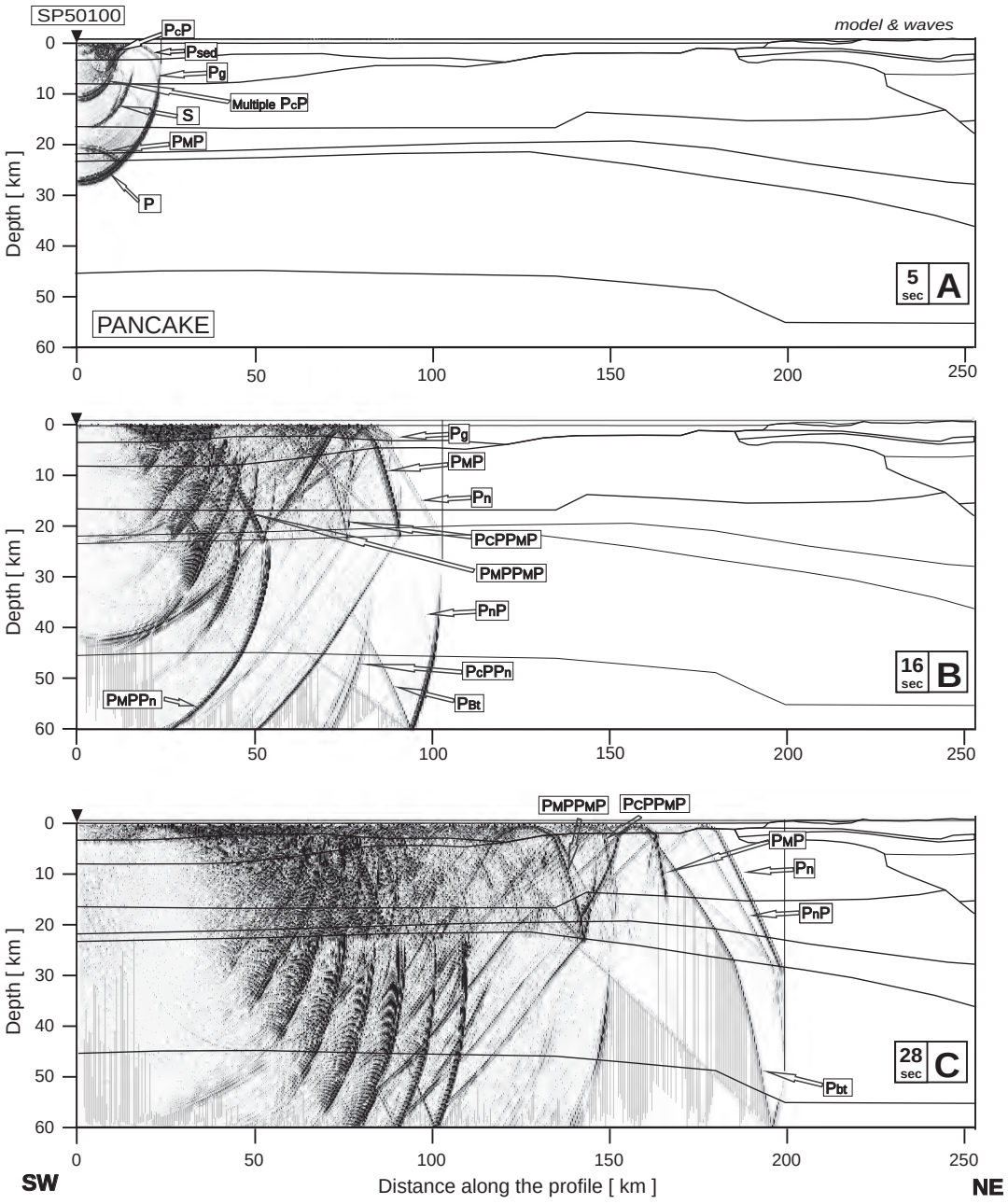


Fig. 10. A series of snapshots of wave propagation in the model from shot point 50100 fixed at 5th, 16th and 28th second after the shot. (A) 5 s after the shot. Direct P-wave travels in sedimentary layers, basement and has reached the mantle. Direct S-wave is clearly observed in the basement. P_MP-wave travels upward after having been reflected from the Moho. The P_cP-wave (reflected from the basement and again from the surface) propagates downward as a secondary strong multiple P_cP-wave. (B) — 16 s after the shot. P_g is ahead of P_{sed} in the first arrivals at distances 84 km. P_n is ahead of P_MP inside the basement but is behind P_g and P_{sed} waves. The P_MP reflection is weak. The P_MP-wave has been reflected back from the surface and once again from the Moho as a multiple (P_MPP_MP) and has initiated a multiple refracted wave in mantle (P_MPP_n). An artificial strong reflection P_{Bt}P from the model bottom is observed. (C) 28 s after the shot. P_n is ahead in the first arrivals at distances 177 km on the surface; P_nP follows immediately after P_n. The artificial reflection from the bottom of the model (P_{Bt}P) is ahead of P_MP inside the crystalline crust but is still behind P_MP near the surface (distance ~ 160 km). Multiple waves P_MPP_MP and P_cPP_MP are observed on the surface at distances ~126 and 143 km respectively.

5.1.3. Profile distance km 380–650

The cratonic crust, from km ~380 (at the surface but km ~260 at the Moho depth) to the north-eastern end of the profile, is considerably thicker than the PB and has a distinct three-layer velocity structure. The sedimentary cover of the EEC, including its Neoproterozoic (Vendian and Riphean) and Palaeozoic sediments, gradually thins north-eastwards from 5 km near the TESZ to near-zero in the Ukrainian Shield. The velocities of 5.1–5.5 km/s recorded in the sedimentary layers are in contrast to previous studies (Sollogub, 1986; Sollogub et al., 1988), which did not observe such low velocities in this region. The Palaeozoic sediments of the Lviv Trough with velocities 5.15–5.28 km/s reach 5 km in thickness at the Rava Ruska fault (in the interval of km 340–350). The Devonian strata, however, have velocities up to 5.95 km/s due to metamorphism in the vicinity of the TESZ and possibly also due to the presence of carbonate rocks. The transition to the Archaean–Mesoproterozoic crystalline basement of the EEC is marked by velocity increase to 6.10–6.20 km/s.

The upper crystalline crust of the EEC (down to depths of 20–25 km) has V_p velocities similar to the upper crust of the Pannonian Basin (6.1–6.3 km/s, Figs 13–17). However, within the EEC at km 320–480 and km 550–630 (the Lviv and Volyn-Podolsk troughs) it includes low velocity lenses (with V_p ~ 6.1 km/s) at depths of 12–18 km and 15–18 km,

Author's Personal Copy

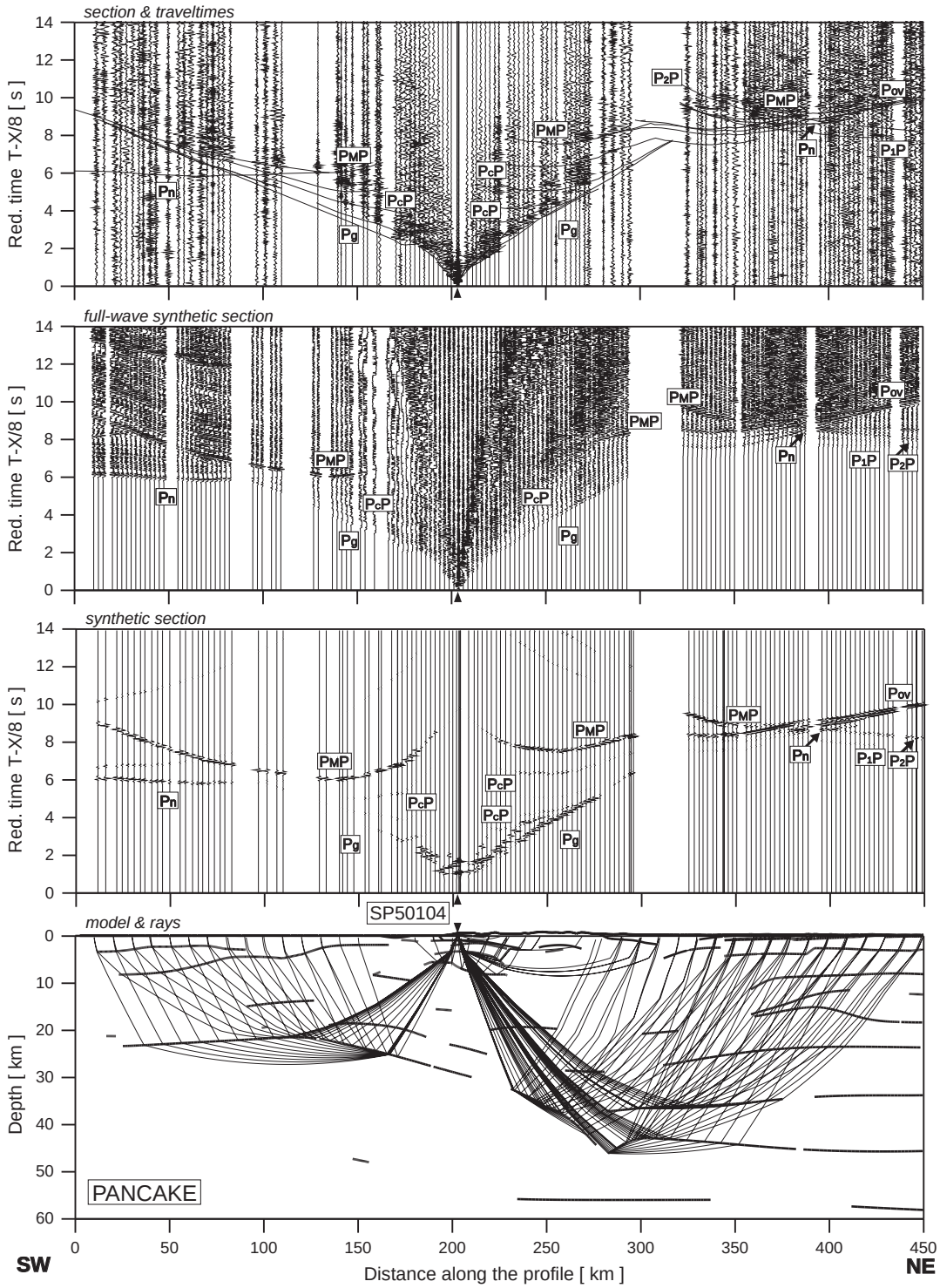


Fig. 11. Example seismic modelling result along the PANCAKE profile, SP50104; seismic record sections (amplitude-normalized vertical component) of P-wave with theoretical travel times calculated using the SEIS83 ray-tracing technique. P-wave data have been filtered using the band-pass filter of 2–15 Hz and displayed using the reduction velocity of 8.0 km/s. Full waveform synthetic seismograms using TESSERAL program (second diagram). Synthetic seismograms (third diagram) and ray diagram of selected rays using the SEIS83 (bottom diagram). All examples were calculated for the model presented in Fig. 7. Other abbreviations are as in Fig. 4.

respectively (Fig. 7). The middle crust in the EEC is slightly faster (V_p = 6.6–6.7 km/s) than in the PB lower crust with a thickness of ~9 km (in depth ranges from 20–25 km to 27–33 km).

In the lower crust (down to Moho at 44–48 km depth), crustal velocities increase to 6.9–7.4 km/s. A strongly reflective, 6–16 km thick, lower crustal layer at depths of ca. 30–48 km can be divided into two parts: a typical lower crustal layer (velocity 6.95 km/s) in the western part of the EEC (km 260–410) and a ca. 5 km thicker high velocity lower crust (HVLC) with V_p = 7.2–7.4 km/s in the east (km 410–590). The high velocities may represent modified lower crust, at least in part, by magmatic underplating or mafic intrusion, as interpreted in other locations worldwide (e.g. Clowes et al., 2002; Korsman et al., 1999; Thybo and Artemieva, 2013). These high lower crustal velocities are constrained only by strong overcritical reflected P_MP phases observed on shot record of SP50113 (the NE end of the profile). The modelling of SP50104 (Fig. 11) shows that V_p in the lower crust cannot

Author's Personal Copy

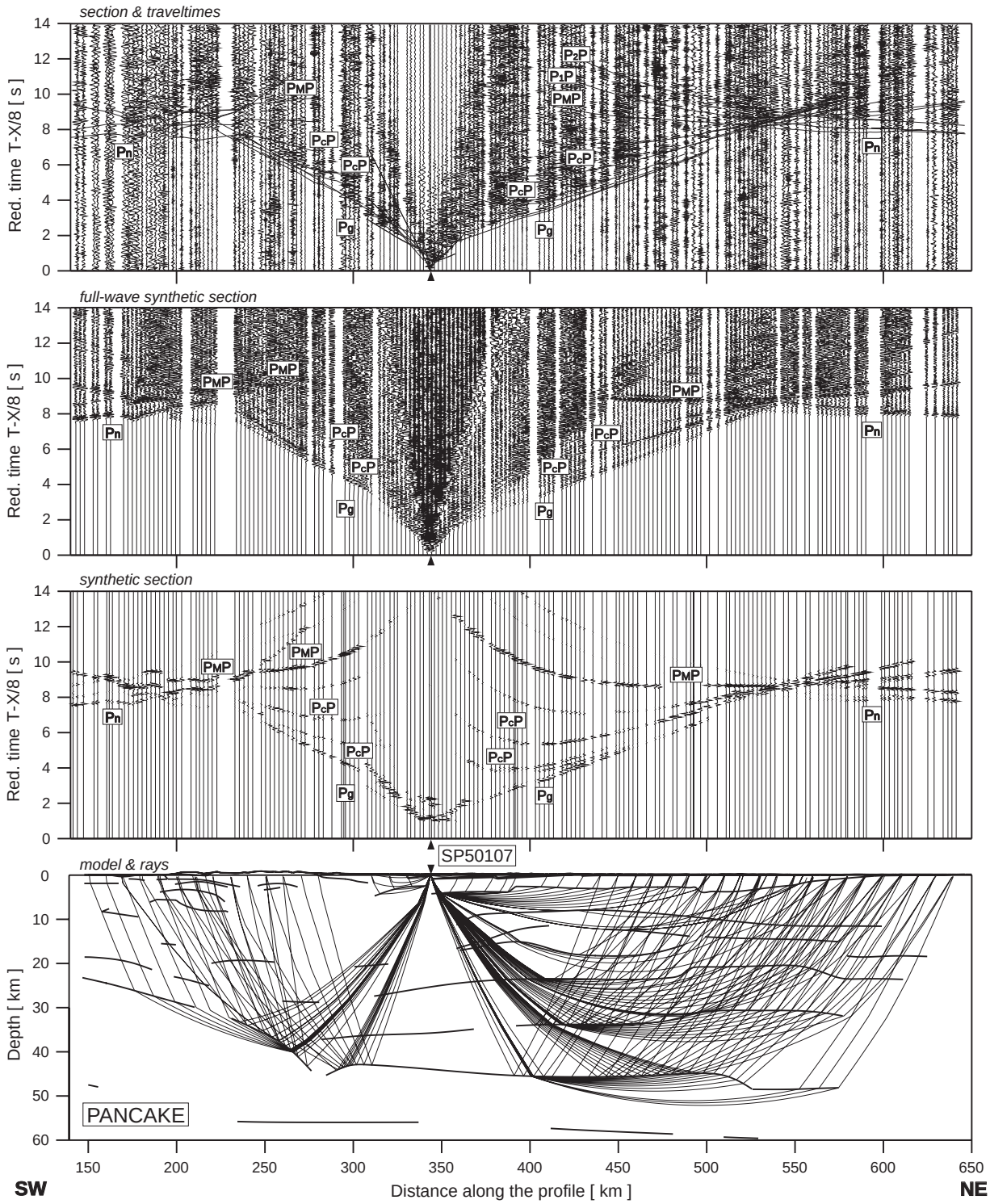


Fig. 12. Example seismic modelling result along the PANCAKE profile, SP50107; seismic record sections (amplitude-normalized vertical component) of P-wave with theoretical travel times calculated using the SEIS83 ray-tracing technique. P-wave data have been filtered using the band-pass filter of 2–15 Hz and displayed using the reduction velocity of 8.0 km/s. Full waveform synthetic seismograms using TESSERAL program (second diagram). Synthetic seismograms (third diagram) and ray diagram of selected rays using the SEIS83 (bottom diagram). All examples were calculated for the model presented in Fig. 7. Other abbreviations are as in Fig. 4.

be higher than 7.0 km/s in the western part of the EEC, but must be ~7.4 km/s in the eastern (HVLC) block (SP50113, Fig. 15).

5.2. Moho boundary and upper mantle velocity

The crust along the PANCAKE profile shows large variations in Moho depth (Fig. 7). In the south-western part of the profile, below the PB and the Transcarpathian Depression, the depth to the Moho is rather uniform (22–25 km). Beneath the Carpathians, the Moho depth changes from 25 to 45 km over a relatively short distance of ca. 100 km. This can be illustrated by the record section of SP50104, where in its north-eastern part two P_MP branches are observed, one at 7.6 s reduced time (km 230–300), and a second with higher apparent velocity at ~9 s (km 330–380) (Fig. 11). As noted before,

Author's Personal Copy

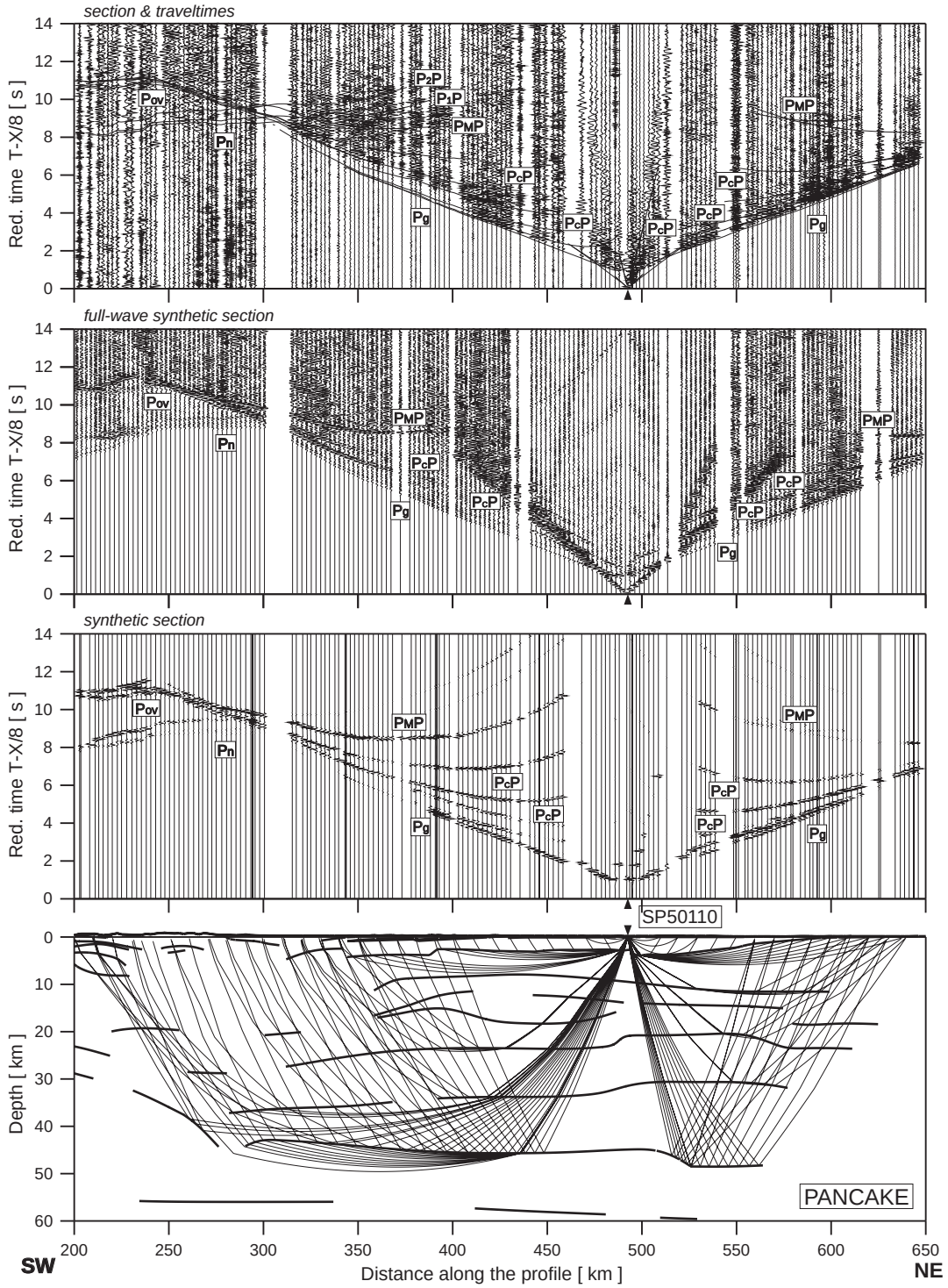


Fig. 13. Example seismic modelling result along the PANCAKE profile, SP50110; seismic record sections (amplitude-normalized vertical component) of P-wave with theoretical travel times calculated using the SEIS83 ray-tracing technique. P-wave data have been filtered using the band-pass filter of 2–15 Hz and displayed using the reduction velocity of 8.0 km/s. Full waveform synthetic seismograms using TESSERAL program (second diagram). Synthetic seismograms (third diagram) and ray diagram of selected rays using the SEIS83 (bottom diagram). All examples were calculated for the model presented in Fig. 7. Other abbreviations are as in Fig. 4.

velocities in the lower crust are based on the overcritically reflected P_MP phases only on record section of SP50104. Therefore, due to the trade-off between the reflector depth and velocity in the overlying layer, the Moho could be up to 4 km deeper if the lower crustal velocity is ~7.2 km/s, but not 6.9 km/s (Fig. 7). Within the EEC and the eastern part of the TESZ, the depth to Moho is uniform and gradually increases from ca. 45 km beneath the Carpathians Foredeep to ca. 40 km in the Volyn-Podolsk block of the Ukrainian Shield.

Similar to the depth to Moho, the sub-Moho velocities are distinctly different beneath the Phanerozoic and cratonic Europe. They are around 8.0 km/s beneath the Pannonian Basin, slightly higher (8.0–8.1 km/s) beneath the Eastern Carpathians, and have values (~8.3 km/s) beneath the EEC.

Several sub-horizontal reflectors in the upper mantle, about 10–20 km below the Moho, are observed beneath the EEC, similar to the findings from the POLONAISE project (Grad et al., 2002), profiles

Author's Personal Copy

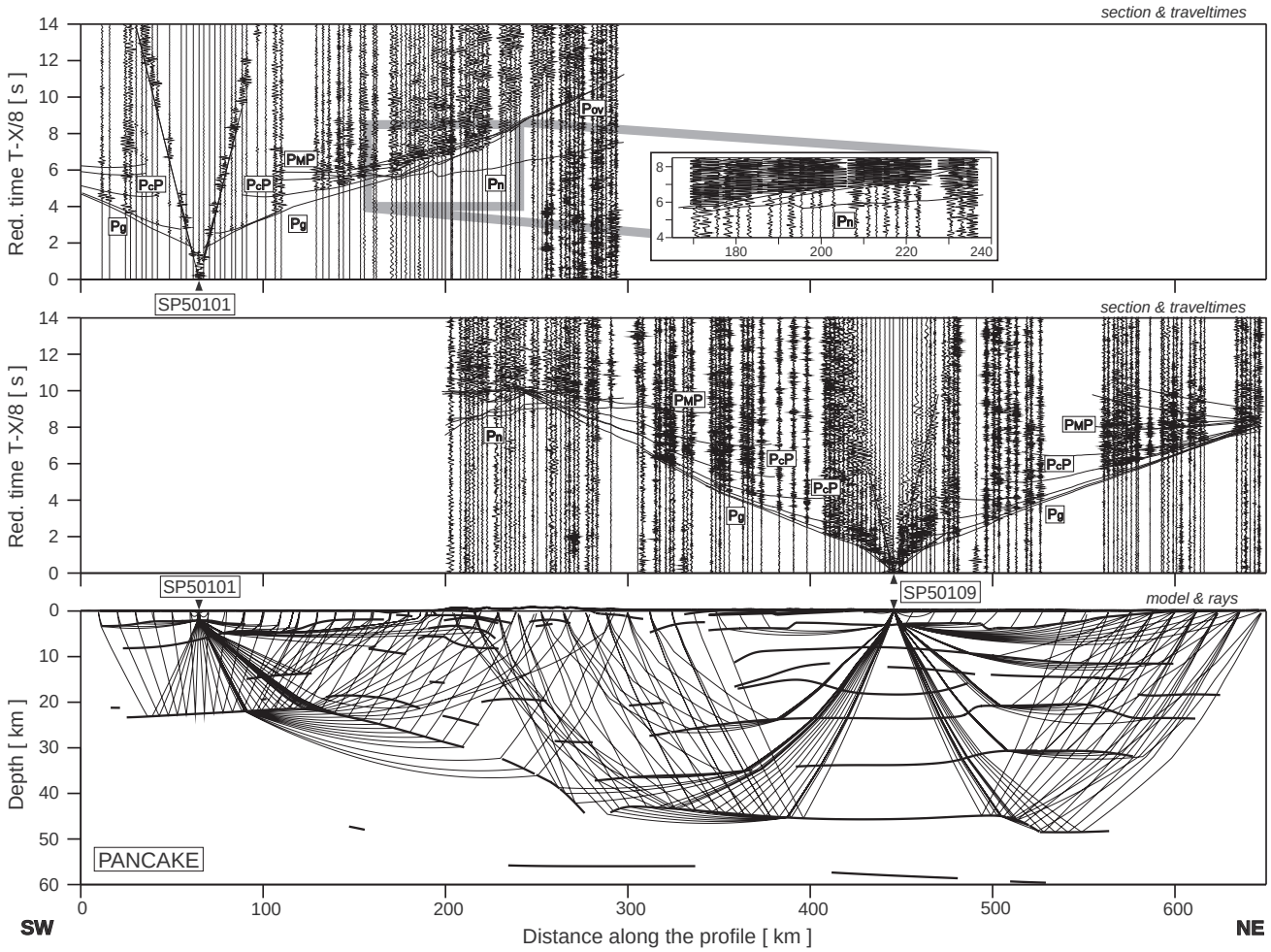


Fig. 14. Example of results derived using the SEIS83 ray-tracing technique for SP50101 and SP50109 of the PANCAKE profile. Amplitude-normalized seismic record section of P-wave with theoretical travel times (top and middle diagrams, respectively), and ray diagrams of P-waves (bottom diagram). Reduction velocity is 8.0 km/s. Other abbreviations are as in Fig. 4.

CEL11 (Janik et al., 2011), CEL04 (Środa et al., 2006) and CEL05 (Grad et al., 2006a) and other cratonic settings (Abramovitz et al, 1997; Artemieva and Meissner, 2012; BABEL WG, 1990). Two reflectors at depths of ~45 km and ~75 km are found below the Pannonian Basin. The upper one is at similar depth as reflectors found on the nearest profiles, CEL04 (Środa et al., 2006) and CEL05 (Grad et al., 2006a).

5.3. Uncertainty analysis of the ray-tracing model

The shot times and locations for shots and receivers are measured with GPS techniques to accuracies of the order of 1 ms and tens of metres, respectively. Such errors are insignificant in a crustal-scale experiment. Uncertainties of velocity and depth constraints in the model obtained by the ray-tracing technique originate primarily from the uncertainties of subjectively picked travel times, which are of the order of 0.1 s for refracted arrivals and up to 200 ms for reflections. However, the uncertainty decreases with improving quality and increasing quantity of data (the number of shots and receivers, the effectiveness of the sources, the signal-to-noise ratio, possibility of checking the reciprocity of the travel time branches, the ray coverage in the model).

Good quality data and careful interpretation has provided a model that produces theoretical travel times fitting the travel time data close to the picking uncertainty, except for the sedimentary and upper mantle reflection phases. Several modelling tests are performed to quantify the uncertainty of the model parameters (Fig. 18). For example, in one test the P-wave velocity in one crustal layer of the final model is perturbed in the range of ± 0.2 km/s; in another test the Moho depth is perturbed by ± 2 km. As it is evident from Fig. 18, the accuracy of the model is better than these values. Similar tests were performed e.g. by Miller et al. (1997) in the Pacific Northwest, and Janik et al. (2002), Grad et al. (2003b), Środa et al. (2006) on POLONAISE and CELEBRATION 2000 data. Diagrams of theoretical and observed travel times, ray coverage and travel time residuals from forward modelling (Fig. 19) show good agreement, with few exceptions. The RMS residual values are 0.10 s for sediments, 0.30 s for the crust, 0.14 s for P_MP, 0.16 s for P_n phases, and 0.59 s for the upper mantle reflections. The RMS residual value is 0.15 s for crustal refracted phases and 0.36 s for reflections. The overall RMS value (for 3905 travel time picks) is 0.32 s.

6. S-wave velocity and V_p/V_s-ratio distribution

The S-wave record sections are prepared with a reduction velocity of 4.52 km/s, a band pass filter of 1–8 Hz and a compressed scale for the time axis with a scale factor of 1.73 compared to the P-wave sections (corresponding to an assumed mean value of $V_p/V_s = 1.73$ for whole crust). These choices allow direct comparison to corresponding P-wave sections with a reduction velocity of 8.0 km/s (Figs 16 and 17). S-wave arrivals were recorded only in the NE part of the profile, and their low quality allows only for a limited number of travel time picks. Although the main secondary and some primary S-wave phases may be picked, with uncertainty, modelling of an independent S-wave velocity model is not possible. Instead, the best quality branches of S-wave travel times are used to estimate the V_p/V_s ratio in the crystalline crust and upper mantle.

Author's Personal Copy

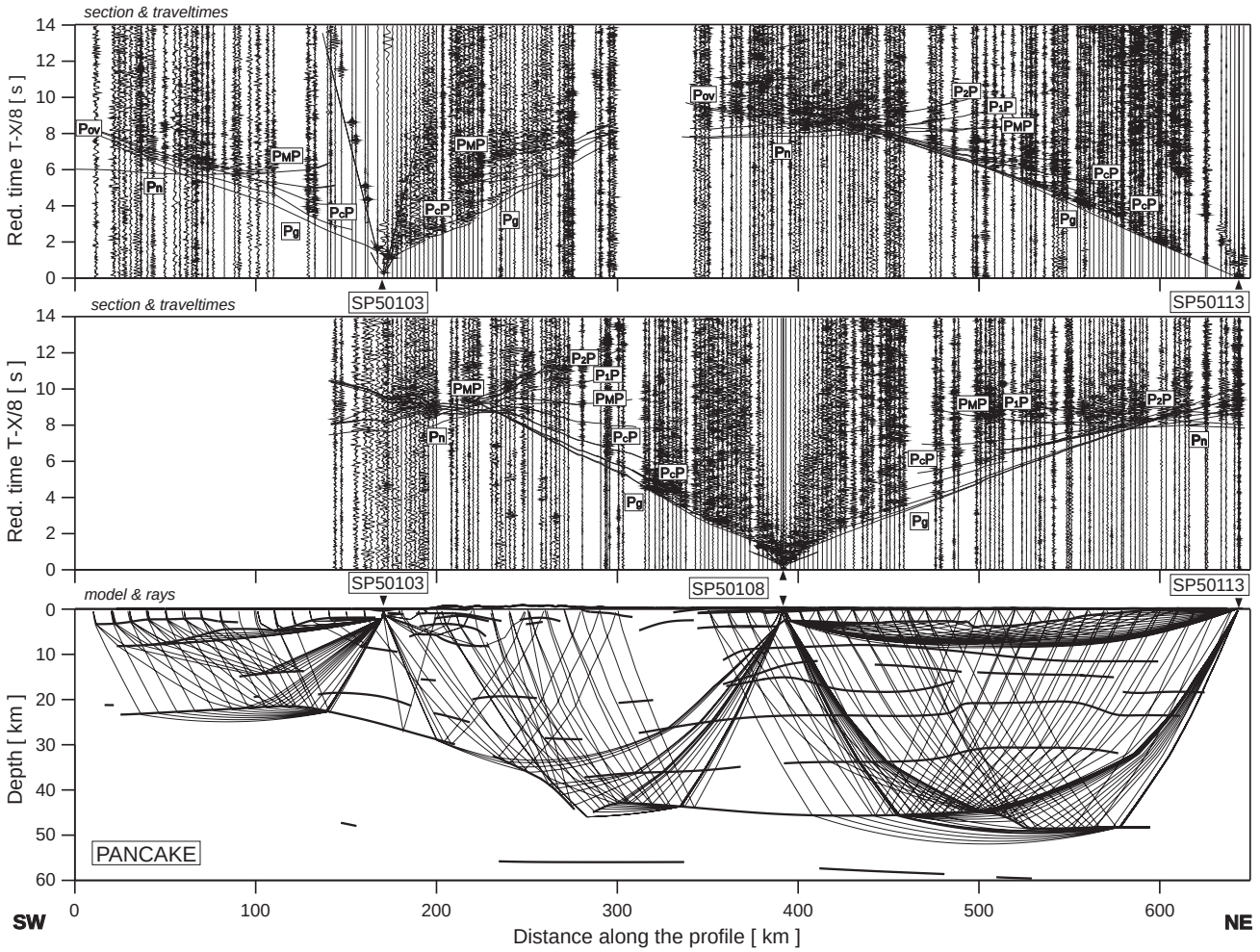


Fig. 15. Example of results derived using the SEIS83 ray-tracing technique for SP50103, SP50108 and SP50113 of the PANCAKE profile. Amplitude-normalized seismic record section of P-wave with theoretical travel times (top and middle diagrams, respectively), and ray diagrams of P-waves (bottom diagram). Reduction velocity is 8.0 km/s. Other abbreviations are as in Fig. 4.

The geometry of discontinuities is assumed the same as in the P-wave velocity model (Fig. 7) and the V_p/V_s ratio is assumed to be constant for each layer of the EEC. Because of the low resolution of the data at small offsets, all layers down to 10–13 km depth are modelled jointly which resulted in a mean ratio of $V_p/V_s = 1.67$. In the deeper layers ($V_p = 6.25$ km/s) $V_p/V_s = 1.73$, and in the middle crust ($V_p \sim 6.6$ km/s) $V_p/V_s = 1.77$. However, in the HVLC ($V_p \sim 7.2$–7.4 km/s), at the north-eastern part of the profile, there are large values of $V_p/V_s = 1.80$. In the sub-Moho mantle, a reliable V_p/V_s estimate cannot be made given unclear S_n arrivals, and a normal V_p/V_s value of ~1.73 was adopted.

7. Tectonic interpretation of the velocity model

The major features of our tectonic interpretation of the velocity model (Fig. 20) are discussed from the Pannonian Basin in the southwest to the Ukrainian Shield in the northeast.

7.1. The Pannonian Basin and the Transcarpathian Depression

For a continental region, the Pannonian Basin has an unusually thin crust, less than 25 km, which is significantly thinner than a global average of ca. 30.5 km for continental extended crust (Christensen and Mooney, 1995). However, the low average basement velocity (ca. 6.1 km/s) provides strong evidence for a continental type of crust. Furthermore, the velocity is smaller than the global average for extended continental crust (6.21 km/s) and significantly smaller than average basement velocity (6.2–6.4 km/s) in the Variscan crust (Aichroth et al, 1992; Artemieva and Meissner, 2012), where a pre-existing mafic lower crust may have been delaminated or thinned to a few kilometres thickness, if still present beneath the crustal blocks. Aarge thickness of sediments could imply an extensional basins; folded Meso-Cenozoic sediments with $V_p = 5.95$ km/s overlying the Palaeozoic basement may represent nappe structures emplaced during the north-eastward convergence of the ALCAPA micro-plate and the EEC. A low-frequency seismic survey (Hajnal et al., 2004) and analysis of upper crustal xenoliths (Kovács et al., 2000) suggest that some parts of the upper crust include deformed metamorphosed rocks of Mesozoic and Palaeozoic age (Haas et al., 2000).

7.2. The Carpathian orogen and the TESZ

The crustal structure of the Carpathian orogen, where crossed by the PANCAKE profile, is unusual in having a 20–21 km thick (meta)sedimentary sequence consisting of three layers with similar thicknesses (with $V_p < 4.65$ km/s down to a depth of 5–7 km, 5.45–5.55 km/s down to a depth of 12–14 km, and $V_p \sim 5.29$ km/s in the bottom part). Analysis of borehole and seismic data from Geotraverse II (Patalakha et al., 2003) suggests that the boundary between the layers with $V_p = 4.60$ and $V_p = 5.50$ km/s (at 4–6 km depth) in the Carpathian Foredeep is likely to represent (approximately) the base of the flysch complex, where it is thrust over older metasedimentary units forming the marginal part of the EEC. Below the Carpathian flysch sediments, the uppermost part of the basement with $V_p = 5.50$ probably comprises Mesozoic cover, including the Cretaceous flysch formations (Zayats and Moroshan, 2007).

Author's Personal Copy

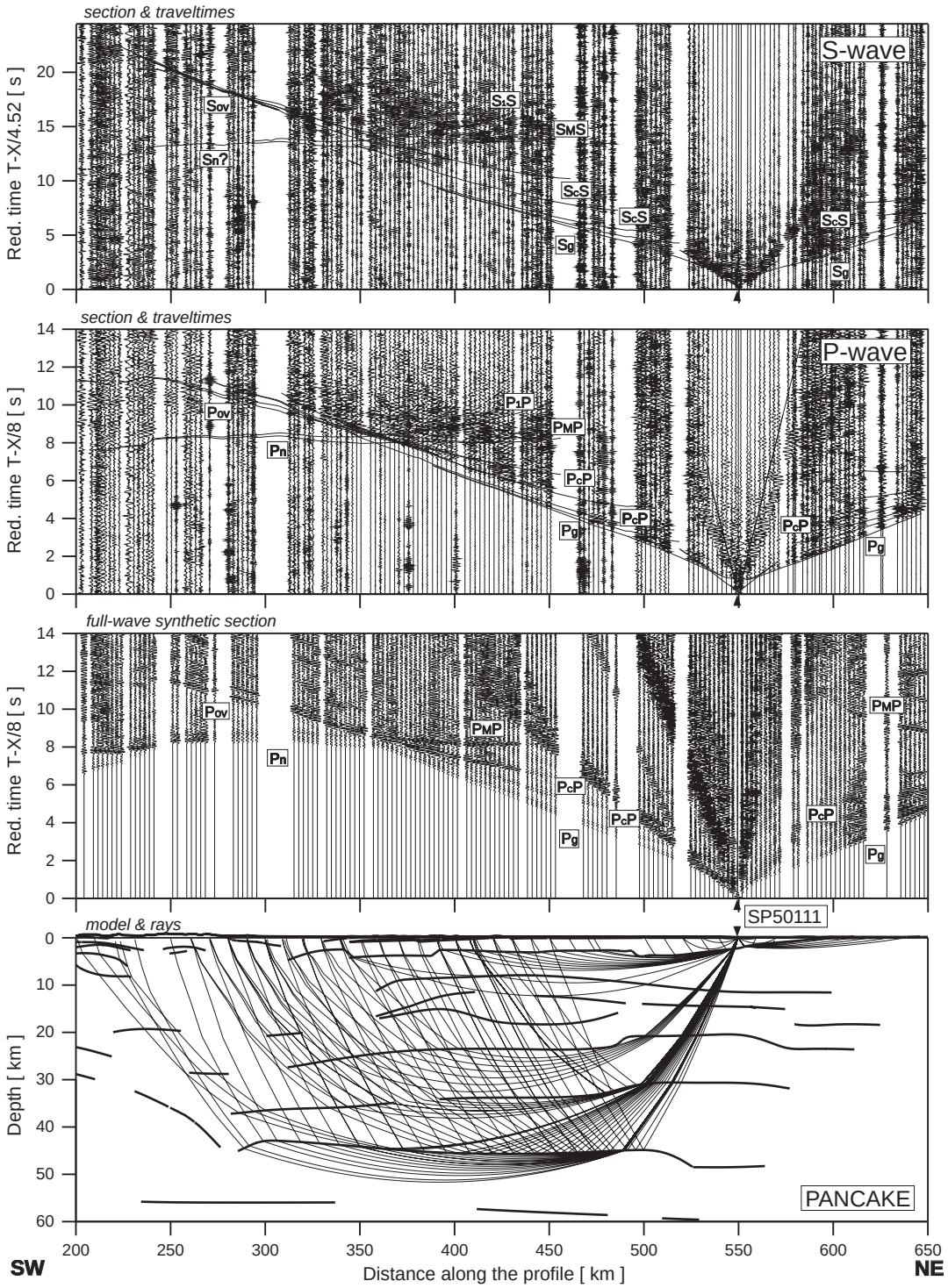


Fig. 16. Example of results derived using the SEIS83 ray-tracing technique for SP50111 of the PANCAKE profile. Amplitude-normalized seismic record section of S- and P-wave with theoretical travel times (top and second diagrams), and ray diagram of P-waves (bottom). Full waveform synthetic seismograms using TESSERAL program (second diagram). All examples were calculated for the model presented in Fig. 7. Abbreviations: Pg, Sg — seismic refractions from the upper and middle crystalline crust; Pov — overcritical crustal reflections; PcP, ScS — reflections from the middle crustal discontinuities; P_MP, S_MS — refracted waves from the Moho boundary; Pn, Sn — refractions from the sub-Moho upper mantle; P_1P — P-wave phases from the upper mantle. The reduction velocities are 8.0 km/s and 4.52 km/s for P- and S-waves, respectively.

$V_p = 5.50$ km/s is similar to velocity in the Neoproterozoic to Palaeozoic sediments and metasediments of the Malopolska Unit at the south-western EEC margin in SE Poland, about 150 km to the north-west of the study area (Środa et al., 2006).

The presence of a 20 km low-velocity sequence beneath the orogen is unusual and must be tectonically associated with the TESZ and the Outer Carpathian nappes.

Similar deep basement depressions are typical for many orogenic belts, but are also common in back-arc basins, rifts, and rifted margins, where sedimentary thicknesses in access of 15–20 km are often observed (Artemieva and Thybo, submitted for publication; Cherepanova et al., 2013; Ivanova et al., 2011; Kostyuchenko and Fedorov, 1998; Maystrenko et al., 2003). A possible interpretation of the presence of a 20 km thick sedimentary cover beneath the Eastern Carpathian orogen

Author's Personal Copy

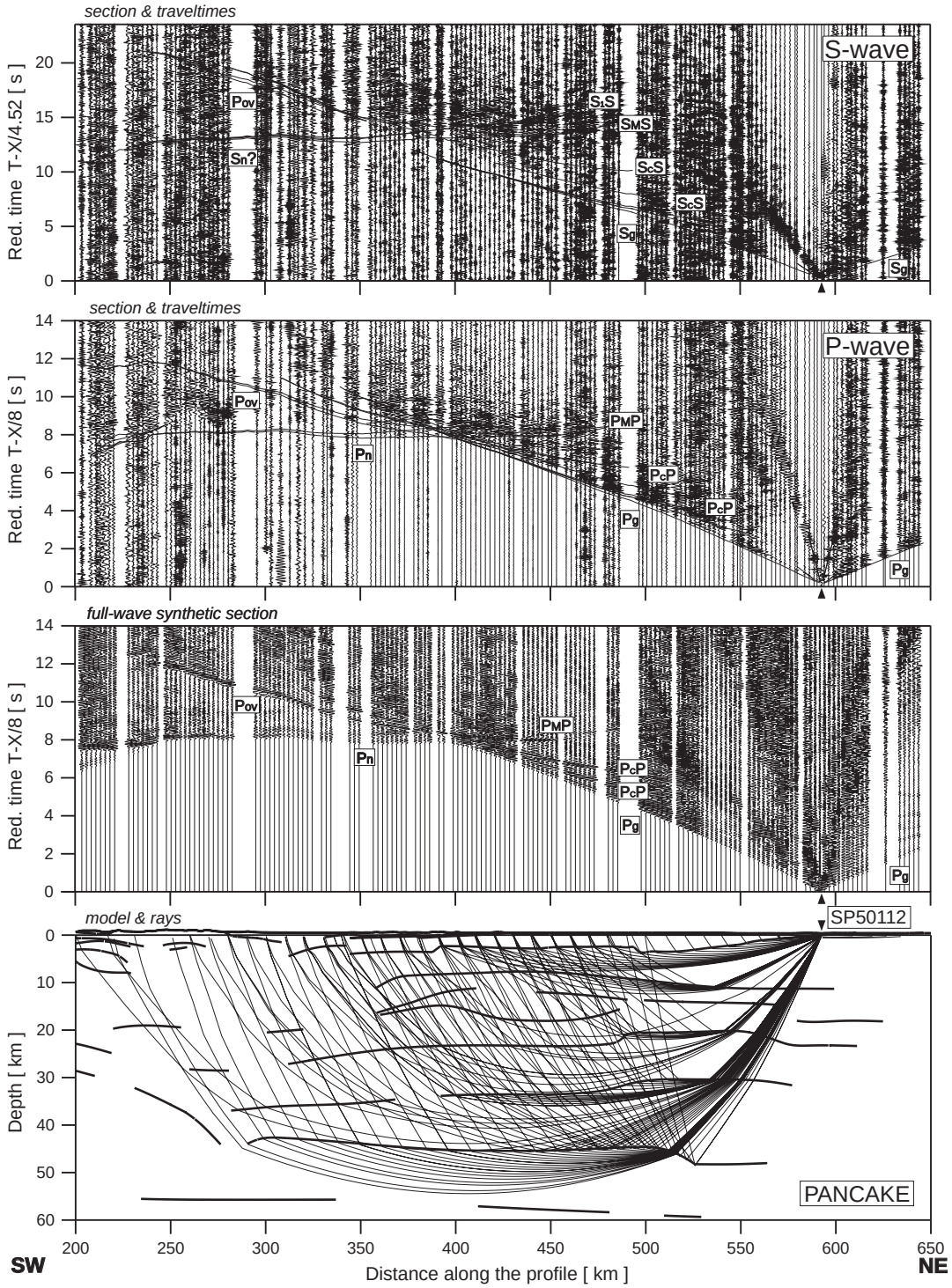


Fig. 17. Example of results derived using the SEIS83 ray-tracing technique for SP50112 of the PANCAKE profile. Amplitude-normalized seismic record section of S- and P-wave with theoretical travel times (top and second diagrams), and ray diagram of P-waves (bottom). Full waveform synthetic seismograms using TESSERAL program (second diagram). Other abbreviations are as in Fig. 16.

includes westward extension of the cratonic upper crust (V_p ~ 6.28 km/s) towards and beneath the Carpathians (depths of 5–20 km at km 280–310, Fig. 7). In this case, the crustal layer at ca. 15–21 km depth with a velocity of 5.29 km/s above thinned EEC crust, may include the autochthonous Vendian-Palaeozoic and Mesozoic cover of the EEC. The layers above may consist of Proterozoic to Palaeozoic (possibly also Mesozoic) metasediments which, in turn, form the basement of the Carpathian flysch nappes.

The crystalline basement of the Carpathian orogen below 20 km depth can be either the old (Proterozoic) basement of the overlying Proterozoic/Palaeozoic units, or alternatively this part of the crust can be either a modified, more reflective ALCAPA crust, or an exotic crustal fragment, preserved after the closure of the Magura Ocean caused by collision of the ALCAPA terrane and the EEC. As compared to the ALCAPA crystalline crust to the south-west, the crust of the Carpathians contains more discontinuities that produce reflected

Author's Personal Copy

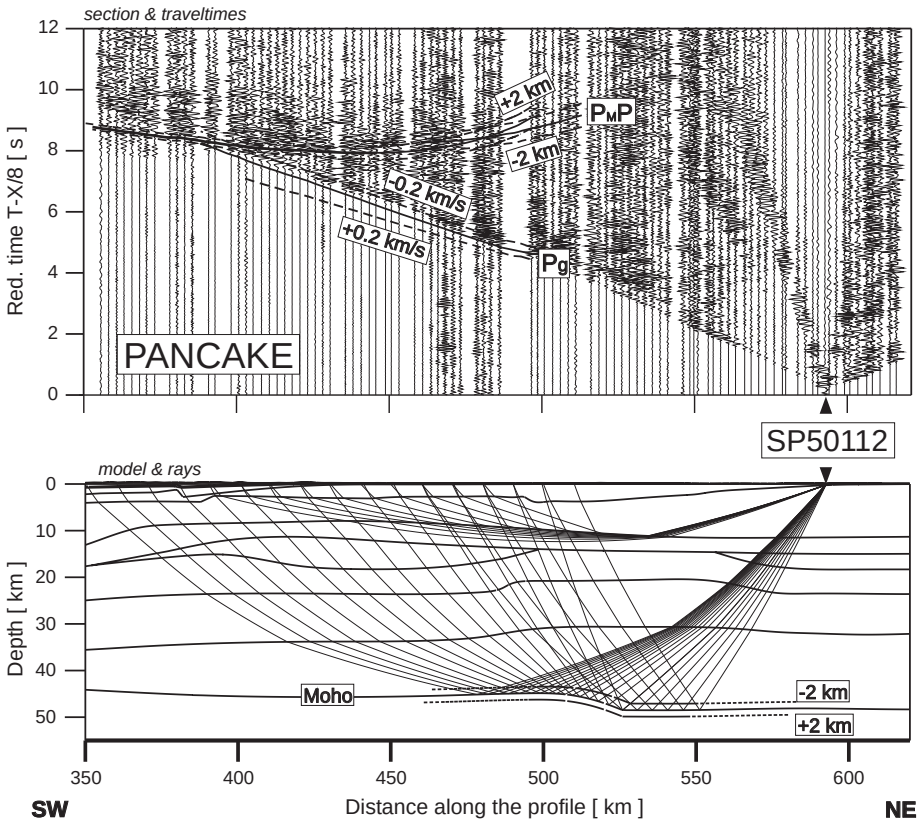


Fig. 18. Seismic record section for shot point 50112 with some Pg and P_MP travel times calculated with perturbed, from the final model, P-wave velocity in one crustal layer (Pg) in the range of ±0.2 km/s as well as separately the Moho depth (P_MP) in the range of ±2 km. Reduction velocity is 8 km/s.

seismic phases, although the velocity distribution is similar. The seismic recordings from this part of the profile are characterized by long codas to the arrivals, as compared to sharp pulses from the ALCAPA crust (Figs. 11–13). However, such codas are observed even for the phases recorded very close to the shot points, which suggests that the apparent reflectivity of the whole crust could also entirely result from large and numerous impedance contrasts in the overlying sedimentary sequences, which overprint the waves emerging out of the crystalline crust with reverberations (see also Jensen et al., 2002).

The Carpathian orogen is unusual in not having a pronounced crustal root (the Moho is at 46–50 km depth which is similar or slightly thinner that the crust to the east). Although the depth to Moho in the Carpathians is similar to the global average for continental orogens (ca. 46 km), most of the Phanerozoic orogens have well documented crustal roots which are distinct features as compared to the adjacent crustal blocks (Artemieva et al., 2006; Cassinis, 2006; Díaz and Gallart, 2009; TRANSALP WG, 2002). Although these orogens are not adjacent to cratonic crust, in contrast to the Carpathians, the Palaeozoic Uralides at the eastern margin of the EEC have a pronounced crustal root, locally down to 55–60 km (Kashubin et al., 2006).

Surprisingly, the TESZ (south of km 340) shows no marked Moho or basement topography. However, there is significant thinning of the crystalline crust of the EEC and thickening of the Proterozoic/Palaeozoic metasedimentary units overlying the EEC margin towards the TESZ (Fig. 7). The Rava Ruska zone marks the north-eastern limit of the TESZ along the profile (Kruglov et al., 2007). According to seismic modelling (km 300–340, Fig. 8), the top of the crystalline basement and other seismic boundaries dip southwestward within the TESZ at an angle of ~15°, which may indicate a low-angle emplacement of the TESZ under the Carpathian orogen. The gravity low (about −90 mGal) over the Carpathian orogen (Fig. 7) has a pointed shape that indicates a narrow zone of low density (and low-velocity) rocks in the upper layers of the crust, which must be associated with a thick sedimentary sequence. An abrupt change in Moho depth (km 260–280) just below this anomaly indicates possible crustal scale deformation around the TESZ in a narrow sub-vertical zone.

7.3. Western margin of the East European Craton

The crystalline crust of the EEC has a three-layered structure typical for cratons worldwide (Fig. 7) (BABEL Working Group, 1993; Beloussov et al., 1991; Clowes et al., 2002; Drummond, 1988; Durrheim and Mooney, 1994; Gintov and Pashkevich, 2010; Grad et al., 2006b; McConnell et al., 1966; Meissner, 1986). Towards the Ukrainian Shield, the cratonic crust gradually thickens in the upper and lower crustal layers, with relatively constant velocities and thicknesses in the middle crust. A high velocity lower crust in the north-eastern part of the profile (km 460–560) coincides with the location of volcanism related to the Pripyat Trough and may imply the presence of intrusive magmatic rocks in the crust.

Two low-velocity lenses at depths of 12–18 km, ca. 3–5 km thick and ca. 100 km long are interpreted beneath the major troughs (Lviv and Volyn-Podolsk) at the western margin of the EEC, between the TESZ and the Ukrainian Shield. Similar low velocity zones in the same depth interval were recognized in the crust of the southern margin of the Siberian craton, the Baikal rift, and the adjacent fold belts by receiver function analysis without information on lateral extent (Zorin et al., 2002). Based on seismic, gravity and geological data, these low velocity zones were interpreted to correspond to thick mylonite zones associated with major thrusts. Since mylonites are highly anisotropic, ductile flow in thrust zones can result in mineral orientation, with high seismic velocities along the foliation direction and minimum velocity in the direction perpendicular to the mylonite foliation. By a direct analogy with the interpretations for Siberia (Zorin et al., 2002), it can be argued that the upper crustal low

Author's Personal Copy

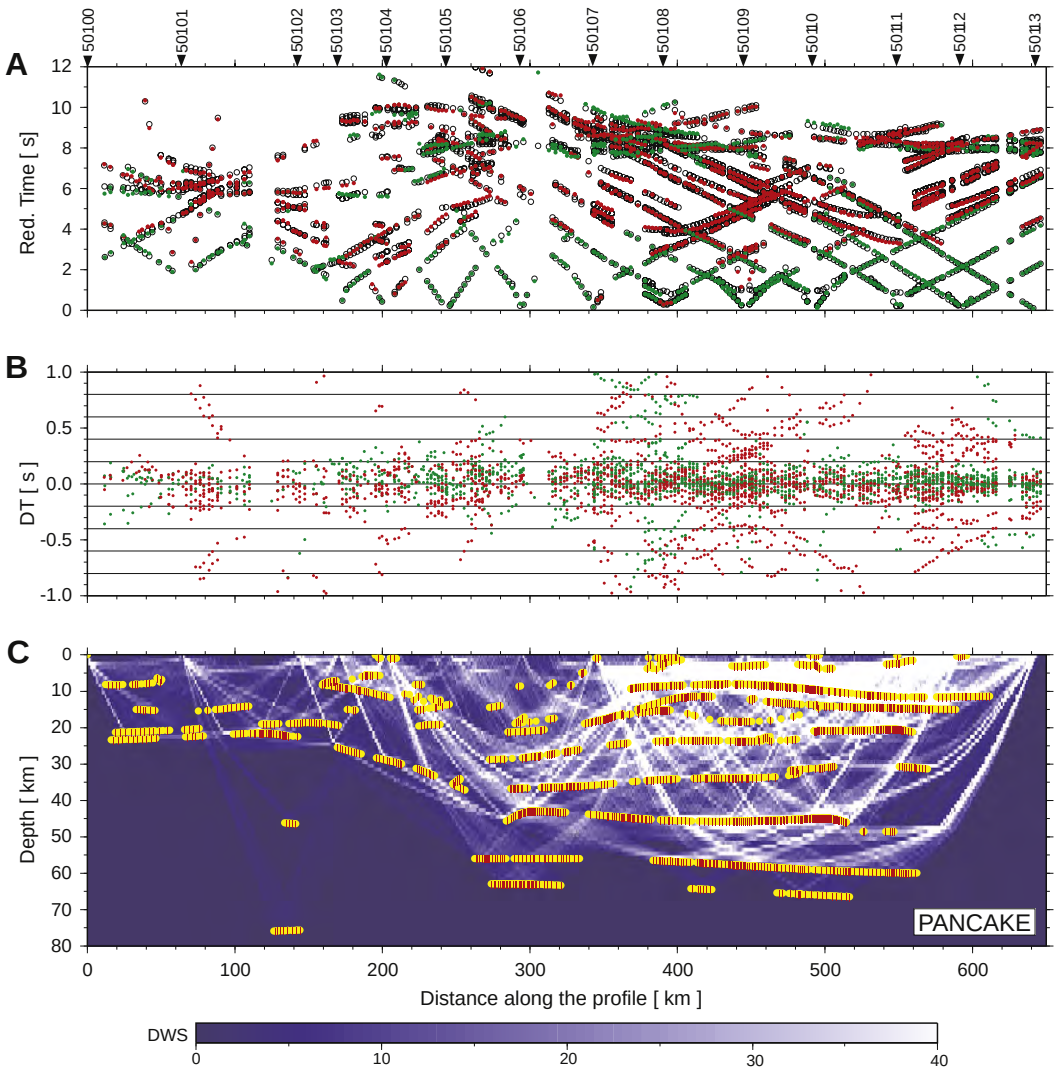


Fig. 19. Diagrams showing theoretical and observed travel times (A), travel time residuals (B) and ray coverage (C) from forward modelling along the profile PANCAKE. Green points — refracted arrivals, red points — reflections, black circles — theoretical travel times. Yellow lines — fragments of discontinuities constrained by reflected phases. The red points plotted along the interfaces mark the bottoming points of the modelled reflected phases (every third point is plotted) and their density is a measure of the positioning accuracy of the reflectors. DWS — derivative weight sum. Reduction velocity is 8 km/s.

velocity layers may mark large thrusts oriented parallel to the TESZ (the direction of ductile flow) in the highly deformed crust at the cratonic margin.

8. Discussion

8.1. The Pannonian Basin and the Transcarpathian Depression

The PANCAKE profile images the crust close to areas of the Pannonian Basin and Carpathians, which were studied previously by the CELEBRATION 2000 profiles (Grad et al., 2006a; Janik et al., 2009, 2011; Środa et al., 2006). These studies, as well as older refraction profiles (Posgay et al., 1978; Sollogub et al., 1988), document a similar crustal structure of the PB to the PANCAKE results, i.e. a 22–30 km thick crust composed of two crystalline layers and a 2–5 km thick sedimentary cover.

Seismic reflectors are identified at depths of 40 and 75 km in the mantle beneath the Pannonian Basin similar to observations in other seismic sections in the Carpathian–Pannonian region (Grad et al., 2006a,b; Janik et al., 2011; Oeberseder et al., 2011; Posgay et al., 1995; Środa et al., 2006). These two horizons may correspond to two lithospheric layers, Kovács et al. (2012) inferred in the ALCAPA lithosphere based on mantle xenoliths. These authors propose that a layer between the Moho and ca. 40 km depth represents old lithosphere that has undergone several deformation events. The deeper layer between 40 and 60–70 km depth may represent juvenile lithosphere added to the older lithosphere by thermal relaxation (cooling) following Miocene extension. This conclusion is in agreement with an independent line of evidence that suggests that during the Miocene extension, solidus temperature (~1000–1100 °C) in the Pannonian Basin may have been reached at a depth of 40 km (Green et al., 2010; Kovács et al., 2012; Kutas, 1993; Kutas et al., 1989), while the present lithosphere–asthenosphere boundary in this region is estimated to be at a depth of 60–70 km (Artemieva et al., 2006; Horváth, 1993; Konecny et al., 2002; Kutas, 1993; Posgay et al., 1995).

8.2. The Carpathians orogen

According to the CELEBRATION 2000 models to the northwest of the PANCAKE profile, in the Outer Carpathians the thickness of the sedimentary nappes increases eastwards, from 8 to 10 km along CEL01 and CEL04 (Środa et al., 2006) to 17–18 km along CEL05 and

Author's Personal Copy

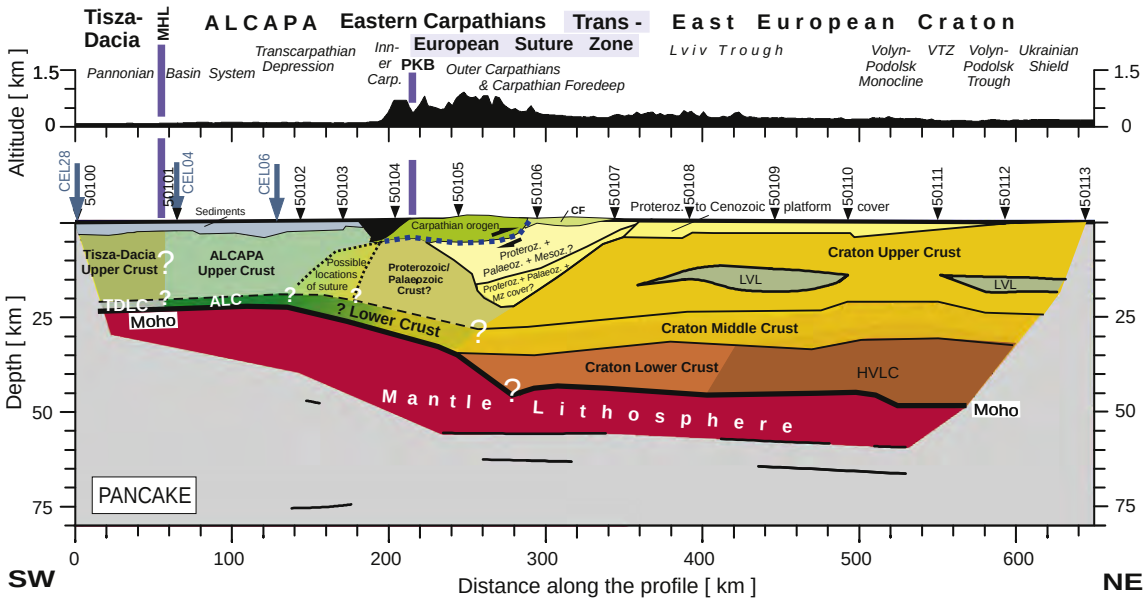


Fig. 20. Tectonic interpretation of the crustal structure along the PANCAKE profile developed by forward ray-tracing, with tectonic interpretation. Thick lines mark velocity discontinuities. Dotted lines mark the supposed suture between the Pannonian Basin structures and the EEC. Abbreviations: ALC — Alcapa lower crust; TDLC — Tisza-Dacia lower crust; CF — Carpathian Foredeep; LVL — low velocity layer; HVLC — high velocity lower crust. Other abbreviations are as in Fig. 7.

CEL11, whereas it is more than 20 km thick along the PANCAKE profile. The difference in the crustal thickness across the Carpathian arc from northwest to southeast is more pronounced for the southern (CEL11, PANCAKE) than for the northern profiles (CEL01, CEL04, CEL05).

According to the results of Geotraverse II (Sollogub et al., 1988), which is sub-parallel and close to the PANCAKE profile (Fig. 1), the greatest depth of the flysch sequences of the Outer Carpathians is 10–14 km, whereas it is only 5–8 km interpreted in the PANCAKE profile. The Geotraverse II model includes the Palaeozoic/Proterozoic basement down to a 20–24 km depth below the inferred flysch layer. This layer apparently corresponds to low velocity metasedimentary strata in the PANCAKE model at similar depths (down to 22 km). The Moho depth in the Geotraverse II model reaches 63 km beneath the Carpathian orogen, which is much deeper than in the PANCAKE model (max 46 km). However, at the depth corresponding to the PANCAKE Moho, the Geotraverse II model includes a velocity discontinuity into a deeper layer with V_p = 7.5–7.6 km/s. These velocities were earlier interpreted as being representative of a mixture of crustal and ultramafic rocks (Sollogub et al., 1988). However, in that study the interpretation of the reflected waves was based on the method of effective parameters (e.g., Egorkin, 1966; Grad, 1983) which cannot provide reliable constraints on the velocities, in particular below reflectors. Given the DSS acquisition conditions, the value of the effective velocity may exceed the value of the mean velocity by as much as 10–15%. The effective depth determined from the reflected wave travel time is also larger than the true depth of the reflecting boundary. The difference increases with increasing distance from the source, and with the DSS data it may exceed 20–30% (Grad, 1983; Janik et al., 2009).

8.3. Western margin of the East European Craton

Profiles CEL11, CEL05 and CEL01 also cross the EEC and Carpathians (Fig. 1) and reveal a three-layered crustal structure and Moho depth >50 km (along CEL05) in the EEC, similar to the central and north-eastern parts of the PANCAKE profile. In the ca. 250 km wide area between the CEL05 and PANCAKE profiles, a shallower Moho (ca. 37 km) was detected where crossed by profiles CEL03, CEL11, CEL13 and CEL14. This area, referred to as the Narol Unit (Janik et al., 2009, 2011; Narkiewicz et al., 2011), is relatively poorly constrained because it is located at the ends of the CELEBRATION 2000 profiles. The PANCAKE data, acquired slightly further to the southeast, do not confirm the presence of thin crust as in the Narol Unit.

V_p/V_s ratio has been estimated on profile EUROBRIDGE'97, which is located ~100 km to the east of the north-eastern end of the PANCAKE profile (Thybo et al., 2003). The V_p/V_s ratio values for upper crust in the PANCAKE model are similar to values for the southern part of the Podolian Block in the EUROBRIDGE'97 model. The PANCAKE values for the middle and high-velocity lower crust correspond to the values for middle and lower crust of the Volyn Block (north of the Podolian Block) from the EUROBRIDGE'97 model. In some places, P-wave velocities and the depth of the Moho boundary are similar on both profiles.

8.4. The EEC–TESZ transition

Our seismic model allows for inferences about the tectonic boundaries (Fig. 20) between the EEC (and adjacent Proterozoic/Palaeozoic units), the Carpathian orogen and the Pannonian Basin structures (ALCAPA micro-plate). According to Fodor et al. (1999) and Horváth (1993) a marine basin that existed between these tectonic units before Neogene time was subducted beneath the Pannonian Basin. However, it is difficult to trace the location of the presumed subduction-related suture, as it was likely obliterated by subsequent tectonic events, including the formation of post-subduction asthenospheric upwelling beneath the PB and collision between the EEC and ALCAPA. The present boundary between these units extends from the surface (at km ~360) to the south-west along the overthrust of the Outer Carpathians over the cratonic margin up to the PKB where, presumably, it continues into the crystalline crust. However, the precise location of this continuation cannot be reliably constrained from the wide angle data (Fig. 20). The data presented in Fig. 8 (km 150–200) suggest the existence of a suture zone between the EEC and the ALCAPA micro-plate (Fig. 20), where V_p velocities (6.18, 6.20, 6.23 km/s) are slightly reduced as compared to the adjacent crust.

CELEBRATION 2000 data indicate that thickening of crust often coincides with the location of thick sedimentary sequences in young tectonic structure of Western Europe which may not be in crustal

Author's Personal Copy

isostatic equilibrium. It has been suggested that the Carpathian orogen and Carpathian Foredeep may have formed by bending of EEC under the ALCAPA and due to the weight of the sedimentary load (Janik et al., 2011). The results of the PANCAKE project indicate that the formation of the Outer Carpathians and their Foredeep cannot be reconciled by such mechanism only, and that more complex models are required for understanding the formation of these units.

According to CELEBRATION 2000 models of the Carpathian lithosphere, the crust at the EEC/ALCAPA contact has almost constant thickness or a moderate crustal root is present (profiles CEL01, CEL04; Środa, 2010; Środa et al., 2006) in the Outer Western Carpathians, where the Palaeozoic units of the TESZ are characterized by a moderate crustal thickness (Małopolska Unit, Bruno-Silesian Unit). In the east (CEL05, CEL11, PANCAKE), where the thick EEC crust reaches close to the Carpathian front, large (> 10 km) variations in the crustal thickness are observed across the Carpathian arc.

However, in the PANCAKE model, these variations are observed not beneath the presumed EEC/ALCAPA contact, but beneath the TESZ. Beneath the contact, the Moho depth increases only moderately, similarly to the Western Carpathians, whereas a substantial increase of depth occurs ~100–120 km further to the north-east. This substantial change in crustal thickness (to ca. 43 km), even if occurring beneath the Outer Eastern Carpathians, is therefore not a result of Carpathian orogenic processes. It is an expression of the old contact of the EEC and Palaeozoic TESZ units, rather than the EEC and the ALCAPA contact.

The Moho depth is constant along the PANCAKE profile beneath the ALCAPA and it does increase to the north-east as indicated from the CELEBRATION 2000 data (Janik et al., 2011). North-eastward deepening of the Moho is observed outside the border of ALCAPA.

9. Conclusions

The 650 km long wide-angle reflection/refraction survey PANCAKE constrains crustal structure across the TESZ. Based on the observed thickness and velocity structure of the crust, profile PANCAKE can be divided into three segments (Fig. 20).

The south-western segment of the profile includes the Pannonian Basin, where the crust is thin (20–25 km with ca. 2–5 km of sediments), lacks any mafic lower crustal layer, and has low average basement velocities (ca. 6.07 km/s and 6.24 km/s, respectively beneath the Pannonian Basin and the Transcarpathian Depression). Upper mantle velocity is ca. 8.0 km/s.

In the central segment (the Outer Eastern Carpathians and the Carpathian Foredeep), the Carpathian orogen may be thrust over the south-western edge of the EEC. The sequences of sedimentary rocks exceed a thickness of 20 km, and includes up to 8 km of the Carpathian flysch above more than 12 km of older metasedimentary rocks. Crustal thickness increases from 22 km to 45 km towards the TESZ, the maximum change of the Moho topography (at km ~240–300, Fig. 20) occurs directly beneath the Proterozoic/Palaeozoic units and their basement, and a lower crustal layer exists only beneath the Outer but not the Inner Carpathians. Beneath the Outer Carpathians and the Carpathians Foredeep, the depth to Moho is almost constant (ca. 44–46 km), which indicates that the orogen does not have a pronounced crustal root.

The north-eastern segment (the EEC) is characterized by a three layered crust with an almost constant crustal thickness (up to 48 km), largely uniform velocity structure and sub-horizontal velocity discontinuities. Low velocity lenses at around 15 km depth are interpreted as thick mylonite zones which mark thrusts oriented parallel to the TESZ (the direction of ductile flow) in the highly deformed crust at the cratonic margin. High-velocity lower crust (7.2–7.4 km/s) around the Ukrainian Shield may represent magmatic intrusions. High upper mantle velocities of 8.3 km/s are typical for cratonic regions.

Subhorizontal mantle reflectors in the lithosphere are observed at depths of 60–70 km beneath the EEC in the north-eastern and central segments of the profile. Two upper mantle reflectors are interpreted beneath the Pannonian Basin at depths of ~45 km and ~75 km.

Acknowledgements

PANCAKE (DOBRE-3) was an international collaboration of institutions and organisations from Ukraine (Institute of Geophysics, National Academy of Sciences of Ukraine, and the State Geophysical Enterprise “Ukrgeofizika”, Kiev), Hungary (Eőtvős Lorand Geophysical Institute, Budapest), Denmark (Department of Geography and Geology, University of Copenhagen), Austria (University of Technology, Vienna), Finland (Institute of Seismology, University of Helsinki), Poland (Institute of Geophysics, Polish Academy of Sciences, and Institute of Geophysics, University of Warsaw), and The Netherlands (Vrie University Amsterdam). The authors offer their sincere thanks to many people who took part in field work and data acquisition. The VU University Amsterdam (ISES) provided financial support for three shot points in Hungary. Tesseral Technologies Inc. developed the software for full waveform modelling. Parallel computations were performed on the SKIT supercomputer hosted at the Glushkov Institute of Cybernetics, National Academy of Science of Ukraine whose staff is acknowledged for providing technical support. The public domain GMT package (Wessel and Smith, 1995) was used to produce some of the maps. The authors are grateful to Prof. G. Randy Keller (The University of Oklahoma, USA) and an anonymous reviewer for helpful comments.

References

Abramovitz, T., Berthelsen, A., Thybo, H., 1997. Proterozoic sutures and terranes in the southeastern Baltic Shield interpreted from BABEL deep seismic data. Tectonophysics 270, 259–277.

Aichroth, B., Prodehl, C., Thybo, H., 1992. Crustal structure along the central segment of the EGT from seismic-refraction studies. Tectonophysics 207, 43–64.

Artemieva, I.M., Meissner, R., 2012. Crustal thickness controlled by plate tectonics: a review of crust–mantle interaction processes illustrated by European examples. Tectonophysics 530–531, 18–49.

Artemieva, I.M., Thybo, H., 2013. Moho discontinuity and crustal structure in Europe, Greenland, and the North Atlantic region. Tectonophysics. http://dx.doi.org/10.1016/j.tecto.2013.08.004 (submitted for publication).

Artemieva, I.M., Thybo, H., Kaban, M.K., 2006. Deep Europe today: geophysical synthesis of the upper mantle structure and lithospheric processes over 3.5 Ga. In: Gee, D.G., Stephenson, R.A. (Eds.), European Lithosphere Dynamics. Geological Society, London, Memoirs, 32, pp. 11–41.

BABEL Working Group, 1990. Evidence for early Proterozoic plate tectonics from seismic reflection profiles in the Baltic Shield. Nature 348, 34–38.

BABEL Working Group, 1993. Deep seismic reflection/refraction interpretation of crustal structure along BABEL profiles A and B in the southern Baltic Sea. Geophysical Journal International 112, 325–343.

Beloussov, V.V., Pavlenkova, N.I., Egorkin, A.V., 1991. Deep Structure of the Territory of the USSR. Nauka, Moscow (224 pp.).

Berthelsen, A., 1993. Were different geological philosophies meet: the Trans-European Suture Zone. Publications of the Institute of Geophysics, Polish Acadamy of Sciences A20 (255), 19–31.

Cassinis, R., 2006. Reviewing pre-TRANSALP DSS models. Tectonophysics 414, 79–86.

Červený, V., Pšenčík, I., 1984. SEIS83 — numerical modelling of seismic wave fields in 2-D laterally varying layered structures by the ray method. In: Engdal, E.R. (Ed.), Documentation of Earthquake Algorithms, Rep. SE-35, World Data Cent. A for Solid Earth Geophysics, Boulder, Colo, pp. 36–40.

Cherepanova, Yu, Artemieva, I.M., Thybo, H., Chemia, Z., 2013. Crustal structure of the Siberian Craton and the West Siberian Basin: an appraisal of existing seismic data. Tectonophysics. http://dx.doi.org/10.1016/j.tecto.2013.05.004.

Christensen, N., Mooney, W., 1995. Seismic velocity structure and composition of the continental crust: a global view. Journal of Geophysical Research 100, 9761–9788.

Cloetingh, S.A.P.L., Burov, E., Matenco, L., 2004. Thermo-mechanical controls on the mode of continental collision in the SE Carpathians (Romania). Earth and Planetary Science Letters 218, 57–76.

Clowes, R.M., Burianyk, M.J.A., Gorman, A.R., et al., 2002. Crustal velocity structure from SAREX, the Southern Alberta Refraction Experiment. Canadian Journal of Earth Sciences 39, 351–373. http://dx.doi.org/10.1139/E01-070.

Csontos, L., Nagymarosy, A., 1998. The mid-Hungarian line: a zone of repeated tectonic inversions. Tectonophysics 297 (1–4), 51–71.

Dadlez, R., 2003. Mesozoic thickness pattern in the Mid-Polish Trough. Geological Quarterly 47 (3), 223–240.

Author's Personal Copy

Dadlez, R., Kowalczewski, Z., Znosko, J., 1994. Some key problems of the pre-Permian tectonics of Poland. Geological Quarterly 38 (2), 169–189.

Díaz, J., Gallart, J., 2009. Crustal structure beneath the Iberian Peninsula and surrounding waters: a new compilation of deep seismic sounding results. Physics of the Earth and Planetary Interiors 173, 181–190.

DOBREfraction'99 Working GroupGrad, M., Grin, D., Guterch, A., Janik, T., Keller, G.R., Lang, R., Lyngsie, S.B., Omelchenko, V., Starostenko, V.I., Stephenson, R.A., Stovba, S.M., Thybo, H., Tolkunov, A., 2003. "DOBREfraction'99" — velocity model of the crust and upper mantle beneath the Donbas Foldbelt (East Ukraine). Tectonophysics 371, 81–110.

Drummond, B.J., 1988. A review of crust/upper mantle structure in the Precambrian areas of Australia and implications for Precambrian crustal evolution. Precambrian Research 40/41, 101–116.

Durrheim, R.J., Mooney, W.D., 1994. Evolution of the Precambrian lithosphere: seismological and geochemical constraints. Journal of Geophysical Research 99, 15,359–15,374.

Egorkin, A.V., 1966. Analysis of the accuracy determination of velocity cross-section in the Earth's crust from travel time of reflected waves. Izvestiya Akademii Nauk SSSR, Fizika Zemli 9, 72–81 (in Russian).

EUROBRIDGE Seismic Working Group, 1999. Seismic velocity structure across the Fennoscandia-Sarmatia suture of the East European Craton beneath the EUROBRIDGE profile through Lithuania and Belarus. Tectonophysics 314, 193–217.

Fodor, L., Csontos, L., Bada, G., Györfi, I., Benkovics, L., 1999. Tertiary tectonic evolution of the Pannonian basin system and neighbouring orogens: a new synthesis of paleostress data. In: Durand, B., Jolivet, L., Horváth, F., Serranne, M. (Eds.), The Mediteranean Basins: Tertiary Extension Within the Alpine Orogen. The Geological Society, London, Special Publications, 156, pp. 295–334.

Fulop, J., Dank, V. eds., 1987. Geological map of Hungary without the Cenozoic cover: Budapest, Hungary, Hungarian Geological Institute, scale 1:500000, 1 sheet.

Gemmer, L., Hauseman, G.A., 2007. Convergence and extension driven by lithospheric gravitational instability: evolution of the Alpine–Carpatian–Pannonian system. Geophysical Journal International 168, 1276–1290.

Gintov, O.B., Pashkevich, I.K., 2010. Tectonophysical analysis and geodynamic interpretation of three-dimensional geophysical model of the Ukrainian Shield. Geophysical Journal (Kiev) 32 (2), 3–27 (in Russian).

Glushko, V.V., Kruglov S.S., 1988. Tectonic map of Ukranian Carpathians 1:500000 (in Russian).

Grad, M., 1983. Determination of mean velocities and depths of boundaries in the Earth's crust from reflected waves. Acta Geophysica Polonica 31, 231–241.

Grad, M., Keller, G.R., Thybo, H., Guterch, A., 2002. Lower lithospheric structure beneath the Trans-European Suture Zone from POLONAISE'97 seismic profiles. Tectonophysics 360, 153–168.

Grad, M., Grin', D., Guterch, A., Keller, R., Lang, R., Lyngsie, S., Lysynchuk, D., Lysynchuk, E., Omelchenko, V., Starostenko, V., Stephenson, R., Stovba, S., Thybo, H., Tolkunov, A., Janik, T., 2003a. DOBRE-99: the crust structure of the Donets Basin along the Mariupol-Belovodsk Profile, Izvestiya. Physics of the Solid Earth 39, 464–473 (Translated from Fizika Zemli, 2003, 6, 33–43).

Grad, M., Jensen, S.L., Keller, G.R., Guterch, A., Thybo, H., Janik, T., Tiira, T., Yliniemi, J., Luosto, U., Motuza, G., Nasedkin, V., Czuba, W., Gaczyński, E., Środa, P., Miller, K.C., Wilde-Piórko, M., Komminaho, K., Jacyna, J., Korabliova, L., 2003b. Crustal structure of the Trans-European suture zone region along POLONAISE'97 seismic profile P4. Journal of Geophysical Research 108 (B11), 2541.

Grad, M., Guterch, A., Keller, G.R., Janik, T., Hegedűs, E., Vozár, J., Ślączka, A., Tiira, T., Yliniemi, J., 2006a. Lithospheric structure beneath trans-Carpathian transect from Precambrian platform to Pannonian basin CELEBRATION 2000 seismic profile CEL05. Journal of Geophysical Research 111, B03301. http://dx.doi.org/10.1029/2005JB003647.

Grad, M., Janik, T., Guterch, A., Środa, P., Czuba, W., EUROBRIDGE'94–97, POLONAISE'97 & CELEBRATION 2000 Seismic Working Groups, 2006b. Lithospheric structure of the western part of the East European Craton investigated by deep seismic profiles. Geological Quarterly 50 (1), 9–22.

Green, D.H., Hibberson, W.O., Kovács, I., Rosenthal, A., 2010. Water and its influence on the lithosphere–asthenosphere boundary. Nature 467, 448–451.

Gursky, D.S. and Kruglov, S.S. (Eds.), 2004. Tectonic Map of the Ukraine M 1:1000000. Edition of State Geological Service, Kiev (in Russian).

Guterch, A., Grad, M., Keller, R.G., 2001. Seismologists celebrate the new millennium with an experiment in Central Europe. EOS 82 (45), 529, 534–535.

Haas, J., Mioč, P., Pamić, J., Tomljenović, B., Árkai, P., Bérczi-Makk, A., Koroknai, B., Kovács, S., Felgenhauer, E.R., 2000. Complex structural pattern of the Alpine–Dinaridic–Pannonian triple junction. International Journal of Earth Sciences 89 (2), 377–389.

Hajnal, Z., Hegedűs, E., Keller, R.G., Fancsik, T., Kovacs, Cs.A., Csabafi, R., 2004. Low-frequency 3-D seismic survey of upper crustal magmatic intrusions in the northeastern Pannonian basin of Hungary. Tectonophysics 388 (1–4), 239–252.

Horváth, F., 1993. Towards a mechanical model for the formation of the Pannonian basin. Tectonophysics 226, 333–357.

Huismans, R.S., Podladchikov, Y.Y., Cloetingh, S.A.P.L., 2001. Dynamic modeling of the transition from passive to active rifting, application to the Pan-nonian basin. Tectonics 20, 1021–1039.

Ivanova, N.M., Sakulina, T.S., Belyaev, I.V., et al., 2011. Depth model of the Barents and Kara seas according to geophysical surveys results. In: Spencer, A.M., Embry, A.F., Gautier, D.L., Stoupakova, A.V., Sørensen, K. (Eds.), Arctic Petroleum Geology. Geol. Soc. London, Memoirs, 35, pp. 209–221. http://dx.doi.org/10.1144/M35.12.

Janik, T., Yliniemi, J., Grad, M., Thybo, H., Tiira, T., POLONAISE P2 Working Group, 2002. Crustal structure across the TESZ along POLONAISE'97 seismic profile P2 in NW Poland. Tectonophysics 360, 129–152.

Janik, T., Grad, M., Guterch, A., CELEBRATION 2000 Working Group, 2009. Seismic structure of the lithosphere between the East European Craton and the Carpathians from the net of CELEBRATION 2000 profiles in SE Poland. Geological Quarterly 53 (1), 141–158.

Janik, T., Grad, M., Guterch, A., Vozár, J., Bielik, M., Vozárova, A., Hegedűs, E., Kovács, C.S., Kovács, I., Keller, G.R., CELEBRATION 2000 Working Group, 2011. Crustal structure of the Western Carpathians and Pannonian Basin: seismic models from CELEBRATION 2000 data and geological implications. Journal of Geodynamics 52, 97–113. http://dx.doi.org/10.1016/j.jog.2010.12.002.

Jensen, S.L., Thybo, H., Polonaise'97 Working Group, 2002. Moho topography and lower crustal wide-angle reflectivity around the TESZ in southern Scandinavia and northeastern Europe. Tectonophysics 360, 187–213.

Kashubin, S., Juhlin, C., Friberg, M., et al., 2006. Crustal structure of the Middle Urals based on seismic reflection data. In: Gee, D.G., Stephenson, R.A. (Eds.), European Lithosphere Dynamics. Geol. Soc. London, Memoirs, 32, pp. 427–442.

Khain, V.E. and Leonov, Yu.G., 1998. International Tectonic Map of Europe, Scale 1:5000000, GIN RAN, Moscow (in Russian).

Khomenko, V.I., 1987. Deep Structure of the South-western Edge of the East-European Platform. Naukova Dumka, Kiev (140 pp., in Russian).

Kolomiyets, A.V., Kharchenko, A.V., 2008. Tuning parallel computations for low-bandwidth network. Computer Mathematics 1, 63–69 (in Russian).

Komminaho, K., 1998. Software Manual for Programs MODEL and XRAYS: A Graphical Interface for SEIS83 Program Package, University of Oulu, Dep. of Geophys., Rep. 20, 31 pp.

Konecny, V., Kovac, M., Lexa, J., Safara, J., 2002. Neogene evolution of the Carpatho-Pannonian region: an interplay of subduction and back-arc diapiric uprise in the mantle. EGU: Stephan Muller Special Publication Series 1, 105–123.

Korsman, K., Korja, T., Pajunen, M., Virransalo, P., GGT/SVEKA Working Group, 1999. The GGT/SVEKA transect: structure and evolution of the continental crust in the Palaeoproterozoic Svecofennian orogen in Finland. International Geology Review 41, 287–333.

Kostyuchenko, S.L., Fedorov, D.L., 1998. Deep structure of Pre-Caspian region and its influence on oil and gas perspectives. Nedra Povolzhiya 16, 6–10 (in Russian).

Kostyukevich, A.S., Starostenko, V.I., Stephenson, R.A., 2000. The full-wave images of the models of the deep lithosphere structures constructed according to DSS and CDP data interpretation. Geophysical Journal (Kiev) 22 (4), 96–98.

Kováč, M., 2000. Geodynamicky, paleograficky a štruktúrny vyvoj karpatsko panónskeho region v miocéne. Novy pohlad na neogénne panvy, Veda, Bratislava (in Slovak), p. 202.

Kováč, M., Král, J., Márton, E., Plašienka, D., Uher, P., 1994. Alpine uplift history of the Central Western Carpathians, geochronological, paleomagnetic, sedimentary and structural data. Geologica Carpathica 45, 83–96.

Kovács, S., Szederkényi, T., Haas, J., Hámor, G., Nagymarosy, A., 2000. Tectonostratigraphic terranes in the pre-neogene basement of the Hungarian part of the Pannonian area. Acta Geologica Hungarica 43 (3), 225–328.

Kovács, I., Falus, Gy, Stuart, G., Hidas, K., Szabó, Cs, Flower, M., Hegedűs, E., Posgay, K., Zilahi-Sebess, L., 2012. Seismic anisotropy and deformation patterns in upper mantle xenoliths from the central Carpathian–Pannonian region: asthenospheric flow as a driving force for Cenozoic extension and extrusion? Tectonophysics 514, 168–179.

Kruglov, S.S., 2001. The problems of tectonics and paleogeodynamics of Western Ukraine (a critical survey of the new publications), Lviv (83 pp.).

Kruglov, S.S., Arsiriy, Yu.O., Bobrov, O.B., Veklich, Ju.M., Velikanov, V.Ya, Vishniakov, I.B., Heychenko, M.V., Gintov, O.B., Yentin, V.A., Znamenskaya, T.O., Lysak, a.M., Lukin, O.Yu., Pashkevych, I.K., Pedanyuk, G.I., Popadyuk, I.V., Poluhtovych, B.M., Radzivill, A.Ya., Rybakov, V.M., Samsonov, V.Y.,Holodnyh, A.B., D.S., 2007. Tectonic map of the Ukraine M 1:1000000. Eds.: Kruglov, S.S. and Gursky, Explanatory note, P.1, Min. of Environment Protection, St. Geol. Survey, Ukr.DGRI, Kiev, 96 pp. (in Russian).

Kutas, R.I., 1993. Analysis of the thermal field and its irregularities. In: Chekunov, A. (Ed.), Lithosphere of Central and Eastern Europe. Summary of the Studies. Naukova Dumka, Kiev, pp. 129–135 (in Russian).

Kutas, R.I., Tsvyashchenko, V.A., Korchagin, I.N., 1989. Heat Flow Modelling of the Continental Lithosphere. Naukova Dumka, Kiev (191 pp., in Russian).

Lyzun, S.O., Zayats, Ch.B., 1997. New data on the deep structure of the Ukrainian Carpathians — geological interpretation of regional seismic profiles. Przegląd Geologiczny 11, 1144–1146 (in Polish).

Maystrenko, Yu., Stovba, S.M., Stephenson, R.A., et al., 2003. Crustal-scale pop-up structure in cratonic lithosphere: DOBRE deep seismic reflection study of the Donbas Foldbelt, Ukraine. Geology 31, 733–736.

McConnell Jr., R.K., Gupta, R.N., Wilson, T., 1966. Compilation of deep crustal seismic refraction profiles. Reviews of Geophysics 4, 41–100.

Meissner, R., 1986. The Continental Crust. Academic Press, Orlando.

Miller, K.C., Keller, G.R., Gridley, J.M., Luetgert, J.H., Mooney, W.D., Thybo, H., 1997. Crustal structure along the west flank of the Cascades, western Washington. Journal of Geophysical Research B Solid Earth and Planets 102, 17,857–17,873.

Narkiewicz, M., Grad, M., Guterch, A., Janik, T., 2011. Crustal Seismic Velocity Structure of Southern Poland: Preserved Memory of a Pre-Devonian Terrane Accretion at the East European Platform Margin, Geol. Mag., 148 (2). Cambridge University Press 191–210. http://dx.doi.org/10.1017/S001675681000049X.

Oeberseder, T., Behm, M., Kovács, I., Falus, G., 2011. A seismic discontinuity in the upper mantle between the Eastern Alps and the Western Carpathians: constraints from wide angle reflections and 3 geological implications. Tectonophysics 504, 122–134.

Patalakha, E.I., Gonchar, V.V., Senchenkov, I.K., Chervinko, O.P., 2003. Geodynamic Elements of the Carpathian Mountains, the Prediction of the Hydrocarbons and Seismic Hazard. EKMO, Kiev (151 pp., in Russian).

Author's Personal Copy

Posgay, K., 1988. The lithosphere structure inside Hungary. The Lithosphere of the Central and East Europe. Geotraverse I, II, V. Naukova Dumka, Kiev, pp. 137–140 (in Russian).

Posgay, K., Salam, A., Mituh, E., Bistrrichan, K., Adam, V., 1978. The Earth's Crust and Upper mantle structure data inside the People Republic of Hungary, in The Earth's Crust and Upper mantle structure of the Central and East Europe. Naukova Dumka, Kiev pp. 35–50 (in Russian).

Posgay, K., Bodoky, T., Hegedűs, E., Kovácsvölgyi, S., Lenkey, L., Szafián, P., Takács, E., Timár, Z., Varga, G., 1995. Asthenospheric structure beneath a Neogene basin in southeast Hungary. Tectonophysics 252, 467–484.

Sollogub, V.B., 1986. The Lithosphere of the Ukraine. Naukova Dumka, Kiev (183 pp., in Russian).

Sollogub, V.B., Chekunov, A.V., Kaluznaya, L.T., 1988. Lithosphere structure along the geotraverse II. Lithosphere of Central and East Europe. Geotraverse I, II, V. Naukova Dumka, Kiev, (63 pp., in Russian).

Środa, P., 2010. The bright spot in the West Carpathian upper mantle: a trace of the Tertiary plate collision — and a caveat for a seismologist. Geophysical Journal International 182, 1–10. http://dx.doi.org/10.1111/j.1365-246X.2010.04595.x.

Środa, P., Czuba, W., Grad, M., Guterch, A., Tokarski, A., Janik, T., Rauch, M., Keller, G.R., Hegedűs, E., Vozár, J., CELEBRATION 2000 Working Group, 2006. Crustal structure of the Western Carpathians from CELEBRATION 2000 profiles CEL01 and CEL04: seismic models and geological implication. Geophysical Journal International 167, 737–760. http://dx.doi.org/10.1111/j.1365-246X.2006.03104.x.

Starostenko, V.I., Grad, M., Gryn, D.N., Guterch, A., Dannovski, A., Kolomiyets, K.V., Legostaeva, O.V., Lysynchuk, D.V., Omelchenko, V.D., Stephenson, R.A., Stratford, W., Thybo, H., Tolkunov, A.P., Flueh, E., Czuba, W., Śhroda, P., Shulgin, A., Janik, T., 2008. Seismic studies of the lithosphere by the DSS and CDP methods at the junction between the East European Platform and the Scythian plates (Project DOBRE-2). Tenth Geoph. Reading by Fedynsky V.V. name, Abstr., Moscow, 41.

Thybo, H., Artemieva, I.M., 2013. Moho and magmatic underplating in continental lithosphere. Tectonophysics. http://dx.doi.org/10.1016/j.tecto.2013.05.032.

Thybo, H., Schonharting, G., 1991. Geophysical evidence for Early Permian igneous activity in a transtensional environment, Denmark. Tectonophysics 189, 193–208.

Thybo, H., Janik, T., Omelchenko, V.D., Grad, M., Garetsky, R.G., Belinsky, A.A., Karatayev, G.I., Zlotski, G., Knudsen, M.E., Sand, R., Yliniemi, J., Tiira, T., Luosto, U., Komminaho, K., Giese, R., Guterch, A., Lund, C.-E., Kharitonov, O.M., Ilchenko, T., Lysynchuk, D.V., Skobelev, V.M., Doody, J.J., 2003. Upper lithospheric seismic velocity structure across the Pripyat Trough and the Ukrainian Shield along the EUROBRIDGE'97 profile. Tectonophysics 371, 41–79.

Tolkunov, A., Sydorenko, G., Voitsytskyi, Z., Starostenko, V., Yegorova, T., Stephenson, R., Omelchenko, V., Pobedash, N., Polyvach, N., 2011. Geological structure of the northwestern terminus of the Eastern Black Sea Rift from new regional CDP profile DOBRE-2. 3rd International Symposium on the Geology of the Black Sea Region, Abstr., Supplement to GEO-ECO-MARINA No.17/2011, Bucharest, Romania, pp. 187–189.

TRANSALP Working Group, 2002. First deep seismic reflection images of the Eastern Alps reveal giant crustal wedges and transcrustal ramps. Geophysical Research Letters 29 (10). http://dx.doi.org/10.1029/2002GRL014911 92-1/92-4.

Wessel, P., Smith, W.H.F., 1995. New version of the Generic Mapping Tools released. EOS, Transactions of the American Geophysical Union 76, 329.

Zaritsky, A.I. (Ed.), 1987. Geological Map of Main Structure Levels in Ukrainian SSR and Moldavian SSR. Scale 1:1000000, Kiev.

Zayats, Ch.B., Moroshan, R.P., 2007. Reserves of oil- and gas-prospective objects in the geological section along transcarpathian geotraverse Uzhok–Borislav–Turka–Rudky–Velyki Mosty. Collected Works UkrDGRI (50 years), 2, pp. 312–316.

Zelt, C.A., 1994. Software Package ZPLOT. Bullard Laboratories, University of Cambridge.

Zorin, Y.A., Mordvinova, V.V., Turutanov, E.K., Belichenko, B.G., Artemyev, A.A., Kosarev, G.L., Gao, S.S., 2002. Low seismic velocity layers in the Earth's crust beneath Eastern Siberia (Russia) and Central Mongolia: receiver function data and their possible geological implication. Tectonophysics 359, 307–327.